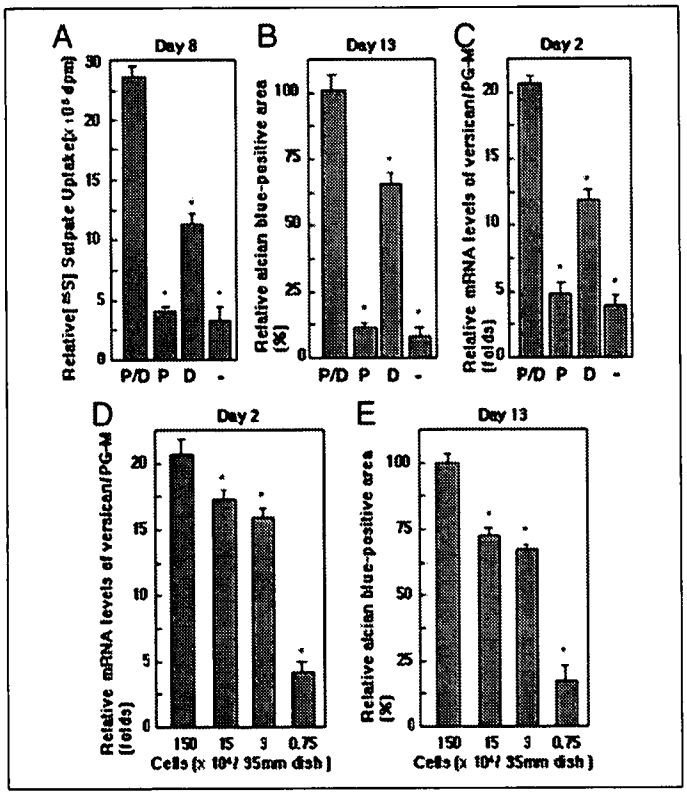

FIGURE 1. **A correlation between early expression of versican/PG-M and later chondrogenesis of N1511 cells.** Chondrogenic differentiation of N1511 cells was induced by treatment with either PTH (*P*) and dexamethasone (*D*) or with both (*P/D*) as described under "Experimental Procedures." The resultant differences of the differentiation were shown by [^{35}S]sulfate incorporation at day 8 (*A*) and Alcian blue-staining at day 13 (*B*). The differences in the expression levels of versican/PG-M were measured by quantitative real time PCR at day 2 (*C*) and well correlated with the differences in the differentiation (*A* and *B*). Chondrogenic differentiation of N1511 cells was also compared by changing the initial cell density from 0.75×10^4 to 150×10^4 cells/dish. The different expression levels of versican/PG-M at day 2 (*D*) were also well correlated with subsequent chondrogenic differentiation measured by Alcian blue-staining at day 13 (*E*), in which the low density culture (0.75×10^4 cells/dish) showed no significant differentiation (compare the degree of staining between the control (no addition) in *B* and 13-day samples). Values were obtained from three independent experiments performed in triplicate (mean ± S.D.; n = 9 in *A*, *C*, and *D*; n = 50 in *B* and *E*). A significant difference from P/D (*A–C*) or 150×10^4 cells/dish (*D* and *E*) was indicated by the *asterisks* (Student's t test; *, $p < 0.01$).

RESULTS

Expression of Versican/PG-M in the Early Phase of Chondrogenesis—We previously optimized the conditions for a novel chondrocytic cell line, N1511, to undergo mesenchymal cell condensation and subsequently chondrocyte differentiation (38). Simultaneous treatment with PTH (P; 1×10^{-7} M) and dexamethasone (D; 1×10^{-6} M) in the presence of 10% serum (P/D) had a maximal effect on the chondrocyte differentiation, but separate treatment in the presence of 10% serum had no effect (PTH or dexamethasone, respectively) (see relative values (per cell) of [^{35}S]sulfate incorporation at day 8 (Fig. 1*A*) and relative values (per cell) of Alcian blue-positive area at day 13 (Fig. 1*B*)). Consistent with those results, P/D treatment brought about a marked expression of versican/PG-M even at day 2, whereas treatment with either PTH or dexamethasone yielded almost the same or higher but not maximal levels of versican/PG-M, compared with the expression without any inducing treatment (−) (see relative mRNA levels of versican/PG-M at day 2, Fig. 1*C*). In this study, all other experiments were performed using the combination treatment of P/D.

We then examined the effect of cell density on the expression. Cells at a density over 3×10^4 cells per 35-mm dish exhibited high levels of versican/PG-M expression at day 2 (Fig. 1*D*) and Alcian blue deposition at day 13 (Fig. 1*E*). On the other hand, cells at a density of 0.75×10^4 cells per 35-mm dish showed the same levels of versican/PG-M at day 2 as those without the inducing treatment and only 15% Alcian blue-positive area of the cells cultured at a high density from the beginning at day 13, although the cells attained the confluency at day 8 (2×10^5 cells per 35-mm dish). Because cell density is known to be a key factor for chondrogenesis, which may reflect the effect of mesenchymal condensation, the possible mechanism could be explained at least in part by the high level expression of versican/PG-M in the cells at high density. Taken together, the results suggest that the chondrogenic effects of the treatment and cell density on N1511 cells involve the strong expression and deposition of versican/PG-M in the early phase.

Changes of Versican/PG-M Expression and Cell Morphology during Chondrogenesis—When N1511 cells were plated at a density of 1.5×10^6 cells/35-mm dish in α-MEM containing 10% FCS, they showed a fibroblastic or polygonal shape. One day later, the cells received the P/D treatment (defined as day 0 at induction). Typical cartilaginous nodules positive for Alcian blue staining and anti-aggrecan antibodies appeared at day 7 and gradually expanded in size with the accumulation of cartilage matrix as described previously (38). By using a well known cartilage development system, chick embryonic limb buds, versican/PG-M has been shown to be highly expressed in the mesenchymal cell condensation area at stage 23 but gradually decreased in an inverse correlation with the increase in the accumulation of aggrecan in the ECM of formed limb cartilage (10, 22, 23). To confirm that N1511 cells also display a sequential expression of versican/PG-M as observed *in vivo*, we performed immunostaining of the cultured cells. The deposition of versican/PG-M started in the ECM soon after plating and, with continuous P/D treatment, became more and more conspicuous at day 2 (Fig. 2, *A* and *B*). When we doubly stained the cells with anti-versican/PG-M antibodies (DAB) and Alcian blue (aggrecan) at day 8, the Alcian blue-stained area in the expanding nodules consistently merged with the versican/PG-M-positive area (Fig. 2*C*).

Northern blot analysis for the cells treated with P/D for several days also showed that the versican/PG-M expression preceded the gene expression of aggrecan (Fig. 2*D*), Col2α1, and Col9α1 (see Fig. 5*A* in Ref. 38). We also performed real time PCR to make a quantitative comparison of the transcription levels of the versican/PG-M and aggrecan genes. Versican/PG-M transcription was up-regulated 21-fold in response to the P/D treatment at day 2, and aggrecan transcription was 16-fold at day 13 (Fig. 2*E*). Without treatment, the cells did not undergo chondrogenesis (38), although they exhibited a transient low level of versican/PG-M expression with a peak at day 1 (data not shown). The results indicated that N1511 cells mimic the *in vivo* expression patterns of versican/PG-M and aggrecan when they receive chondrogenic stimuli, and the strong and temporal expression of versican/PG-M may be an essential step for the subsequent differentiation into chondrocytes. Together with all the results in the former section, N1511 cells could be considered an *in vitro* model system for studying the role of versican/PG-M in chondrogenesis, although it is still unclear how well the system mimics mesenchymal condensation prior to chondrogenesis *in vivo*.

Inhibition by Antisense RNA of Versican/PG-M Synthesis Resulting in Suppression of Chondrogenic Differentiation in N1511 Cells—We next investigated how the expression of versican/PG-M is important for subsequent chondrocyte differentiation using a number of antisense-, sense-, and mock-transfected stable clones (93 antisense, 15 sense, and 94 mock clones). Each individual stable clone was stained with anti-versican/PG-M antibodies for the CS-β domain of versican/PG-M at day 1, and the deposition level of it was measured by NIH image as described under "Experimental Procedures." We then classified stable

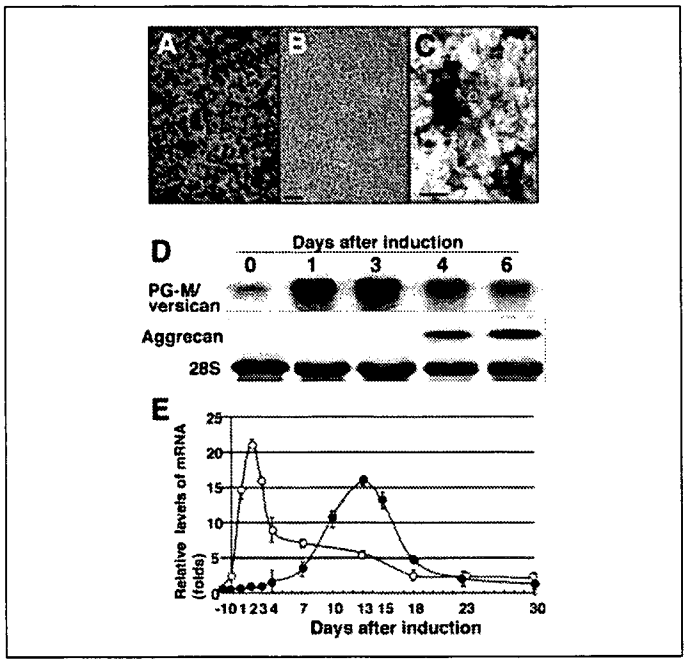

FIGURE 2. **Changes of versican/PG-M expression and cell morphology during the chondrogenic differentiation of N1511 cells.** When N1511 cells are induced as described under "Experimental Procedures," the cells proliferated and elaborated the ECM containing versican/PG-M shown by immunofluorescent staining of cells at day 2 with anti-mouse CS-β domain antibodies (*A* and *B* is phase-contrast images of *A*). The simultaneous accumulation of versican/PG-M and aggrecan in the culture at day 8 were doubly stained with DAB and Alcian blue (*C*). *Bars*, 100 μm. *D*, Northern blot analyses of versican/PG-M and aggrecan gene expression in N1511 cells at the indicated culture days after induction. The gene for versican/PG-M was expressed earlier than the genes for aggrecan. The results shown are representative of three independent experiments with similar results. *E*, changes in transcriptional levels of versican/PG-M (*open circle*) and aggrecan (*solid circle*) measured by quantitative real time PCR during the chondrogenesis. Results were normalized using the GAPDH transcription levels. Each point was the mean ± S.D. obtained from three independent experiments in triplicate (n = 9).

clones into three groups according to their deposition levels shown in Table 1 (group I, no reduction; group II, moderate reduction; and group III, severe reduction). Most of the sense and mock transfectants were in group I, which showed similar levels of versican/PG-M deposition to the parental N1511 cells. In response to the change of versican/PG-M deposition among these three groups shown in TABLE ONE, chondrogenesis was studied by Alcian blue staining, and relative values (per cell) of the positive areas are measured by NIH image at day 18 (Fig. 3*A*). Antisense transfectants of the group II (AS-II) and group III (AS-III) showed dramatic reduction of the aggrecan accumulation up to 48 and 62%, respectively, compared with the parental N1511 cells (valued as 100%), whereas most of the sense and mock transfectants showed no significant reduction (Fig. 3*A*). Among the antisense clones shown in TABLE ONE, we chose 21 clones (seven clones typically representative of each group), and we examined the accumulation in the ECM of versican/PG-M and aggrecan by double staining with DAB and Alcian blue at day 0, 2, 4, 7, 10, 13, and 18. Staining patterns of a representative clone in AS-III, A75, and those in a mock-transfectant, M10 (see Fig. 3*B* as typical examples), demonstrate that the accumulation of versican/PG-M in the matrix always precedes that of aggrecan, and the reduced accumulation of versican/PG-M decreased with aggrecan. The statistical treatment of the results obtained from clones of the three groups with different levels of versican/PG-M deposition clearly showed that reduction in PG-M expression results in reduced aggrecan and that the inhibition of aggrecan deposition depended upon the reduced patterns of versican/PG-M deposition (see those of AS-I, AS-II, and AS-III in Fig. 3*C*). Time-dependent changes in the transcriptional levels of versican/PG-M and aggrecan in the antisense clone A45 in AS-II were measured by quantitative real time PCR during the inhibition of chondrogenesis by the antisense RNA (Fig. 3*D*) (compare with Fig. 2*E*). Based on these data, such a relationship may exist that the suppressed deposition of versican/PG-M was because of the suppressed expression by antisense cDNA transfection and resulted in decreased levels of aggrecan mRNA. Two antisense clones, A12 and A39, in AS-III showed almost no expression of versican/PG-M at the transcriptional level, and these clones showed neither Alcian blue-positive areas nor the expression of the aggrecan transcript (data not shown). The expression of the Col2a1 transcript was also severely suppressed in those clones (data not shown). These results suggest that transient high versican/PG-M expression in the early phase is greatly involved in the chondrogenic differentiation.

TABLE 1

Numbers and versican/PG-M deposition levels of stable clones of antisense, sense, and mock transfectants

Clones of antisense, sense, and mock stable transfectants were isolated as described under "Experimental Procedures." Number of independent clones from the respective transfectants was shown below. Each exhibited the different level of versican/PG-M deposition measured by NIH image after immunostaining with polyclonal antibodies for CS-β domain of versican/PG-M at day 1 as described under "Experimental Procedures." According to their levels, the clones were classified into three groups (group I, no reduction; group II, moderate reduction; group III, severe reduction).

Transfectants	Antisense	Sense	Mock
Versican/PG-M deposition levels			
Group I	35	14	84
Group II	30	1	8
Group III	28	0	2
Total no. of clones	93	15	94

V0 and V1, Major Forms of Versican/PG-M in the Early Phase of Chondrogenesis—Versican/PG-M has been shown by multiple alternative splicing to have four variant forms with different numbers of attached chondroitin sulfate chains as follows: V0, V1, V2, and V3 (Fig. 4*A*). The versican/PG-M expressed in N1511 cells after the chondrogenic induction must be V0 and/or V1 forms because antibodies used for the staining are specific to the CS-β domain, which only the V0 and V1 forms have (16, 20, 44). RT-PCR revealed that N1511 cells in the early phases after chondrogenic induction express mainly V0 at day 1 and V0/V1 at day 4 (Fig. 4*B*). Most interestingly, those cells at day 13, when most cells have already differentiated into chondrocytes, express the V2 form. The smallest form, V3 (20), was not detected at any stage (data not shown). Considering that the CS-β domain is larger in size and richer in potential chondroitin sulfate-attachment sites than the CS-α domain, it is plausible that the V0 and V1 forms have more chondroitin sulfate chains than the V2 form. Therefore, we hypothesized that the chondroitin sulfate chains themselves play an important role in the early phase of chondrocyte differentiation and, if the early phase reflects the case *in vivo*, in the mesenchymal condensation.

Possible Involvement of Chondroitin Sulfate Chains in Chondrocyte Differentiation—We showed previously that chondroitin sulfate chains immobilized to the substrate matrix inhibit the cell-spreading process of cell adhesion (28, 32). It is therefore likely that the chondroitin sulfate chains themselves of versican/PG-M are implicated in the early phase of chondrocyte differentiation where they may have a mesenchymal condensation-like effect by inhibiting cell adhesion. Thus, we first examined the effect of chondroitinase ABC, which degrades the chondroitin sulfate chains of proteoglycans, including versican/PG-M, and leaves the core proteins in the ECM. When added to the culture in the early phase of chondrogenesis (day 0–4), chondroitinase ABC (5 units/ml) fully degraded the chondroitin sulfate chains of versican/PG-M (Fig. 5*A*). It should be noted that the treatment with chondroitinase ABC was only for the initial 4 days of culture, during which the aggrecan expres-

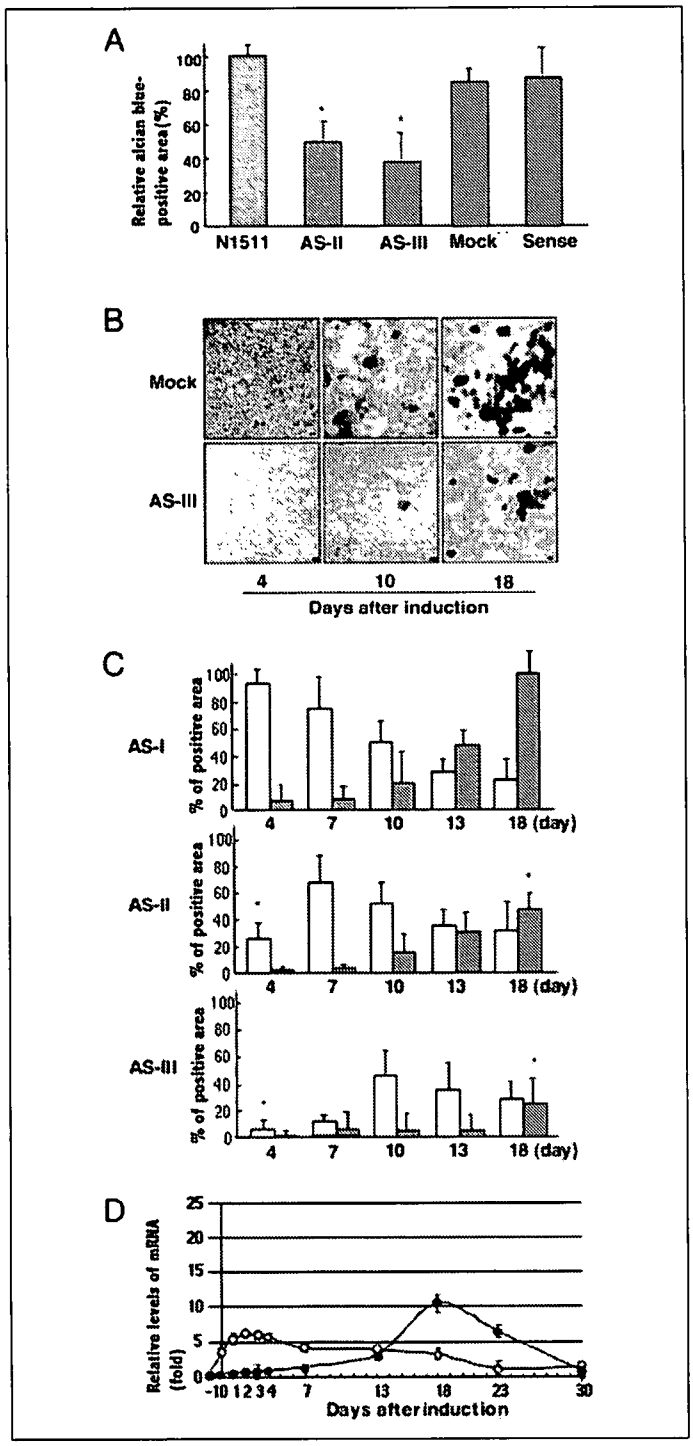

FIGURE 3. **Inhibition of chondrogenic differentiation of N1511 cells by antisense RNA expression of versican/PG-M.** *A*, at day 18, the Alcian blue-positive areas of all the stable clones for antisense, sense, and mock transfectants and those of the parental N1511 cells were quantified as relative values for comparison of the chondrogenic differentiation as described under "Experimental Procedures." *AS-II* and *AS-III*, antisense clones at moderate and severe reduction levels which belonged to group II and group III, respectively (see TABLE ONE), showed dramatic inhibition of chondrogenesis up to 48 and 62%, respectively. Percent values ± S.D. were obtained from the mean ± S.D. of relative measurements of each clone in three independent experiments ($n = 50$), compared with those of the parental N1511 cells which was set as 100%. The *asterisks* indicate $p < 0.001$ in comparison with the parental group, using Student's *t* test. *B*, typical staining patterns of a representative clone of the AS-III, A75, and that of a mock-transfectant (*Mock*), M10, shown by double staining for versican/PG-M and aggrecan with DAB and Alcian blue, respectively. *Bars*, 100 μm. *C*, quantified time-dependent changes of versican/PG-M and aggrecan accumulations (*white* and *gray bars*, respectively) in the antisense-transfectant stable clones at different reduction levels (15 clones, 15 clones, and 14 clones from AS-I, AS-II, and As-III, respectively, see Table 1). Versican/PG-M and aggrecan in each clone were doubly stained, and their accumulations were quantified using NIH image software. The levels of versican/PG-M and aggrecan in parental N1511 cells at day 4 and day 18, respectively, were defined as 100%. Percent values ± S.D. were obtained from triplicate analyses of three independent experiments of representative clones in each group at the indicated days ($n = 9$). The *asterisks* indicate $p < 0.05$ in comparison with the parental N1511 at day 4 for versican/PG-M and at day 18 for aggrecan, respectively, using Student's *t* test. *D*, changes in transcriptional levels of versican/PG-M (*open circle*) and aggrecan (*solid circle*) in the antisense clone, A45 in AS-II, were measured by quantitative real time PCR during the inhibition of chondrogenesis by the antisense RNA (compare with Fig. 2*E*). Values were normalized using the GAPDH transcriptional levels. Each point was the mean ± S.D. obtained from three independent experiments performed in triplicate ($n = 9$).

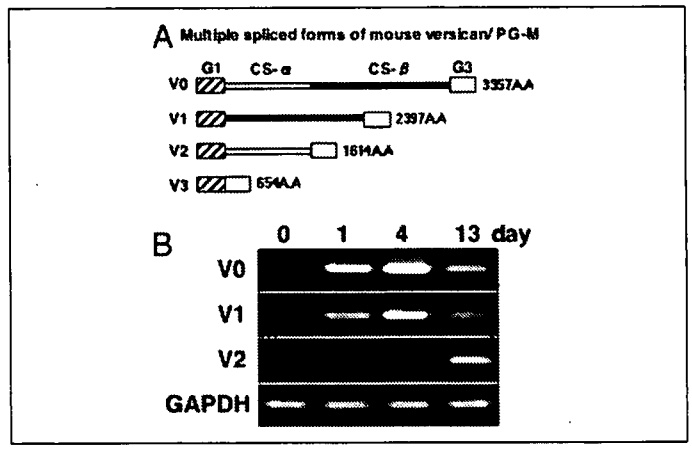

FIGURE 4. **Expression of V0 and V1 variants of versican/PG-M as major forms in the early phase of chondrogenesis.** *A*, four splicing variant forms of versican/PG-M, V0, V1, V2, and V3 (40). The variants are formed by the alternative splicing of two different chondroitin sulfate-binding domains (CS-α and CS-β). *B*, RT-PCR analysis for time-dependent alterations of the four versican/PG-M forms after the chondrogenic induction of N1511 cells. V0 was mainly expressed at day 1, V0/V1 at day 4, and V2 at day 13. V3 was not expressed at any stage. Data are representative of three independent experiments with similar results.

sion was not detected. However, it caused a marked decrease in the accumulation of aggrecan in the ECM by up to 50%, compared with the control culture (defined as 100%) after subsequent culture for a further 2 weeks (at day 18) (Fig. 5*B*), although the treated cultures did not give core bands stained with anti-aggrecan antibodies on the blotting membranes on any culture days (data not shown). When measured by real time quantitative RT-PCR 1 week after the subsequent culture (at day 13), the relative transcription level of aggrecan in the treated culture showed a 30% reduction compared with the normal culture (Fig. 5*C*).

We demonstrated previously that β-xylosides with some of hydrophobic aglycons penetrated into the cells and acted as the artificial initiators for the chondroitin sulfate synthesis (42) to inhibit the native synthesis of chondroitin sulfate chain attached to the core proteins by depriving the synthetic machinery such as enzymes and precursor nucleotides (47). The inhibition is apparently dependent on the concentrations of β-xyloside, although many other factors appeared to be involved in the effect (47). In addition, it has also been shown that β-xyloside treatment of chick embryos *in ovo* induced a decrease in the growth rate of cartilage (42). Thus, we next examined the effect of treatment with various concentrations of β-xyloside in a culture where the treatment was expected for the cells to produce versican/PG-M with lesser chondroitin sulfate. When added to the culture in the early phase of chondrogenesis (day 0–5), the amounts of CS recovered in cell layers were decreased at the concentration over 1.0 mM (Fig. 6*A*), whereas the amounts of CS in culture media were not altered at the concentrations from 0.05 to 2.0 mM (Fig. 6*B*). The CS in cell layer could reflect the native CS synthesized on the core proteins, and the one in media could include CS initiated by β-xyloside. In culture treated with β-xyloside at the

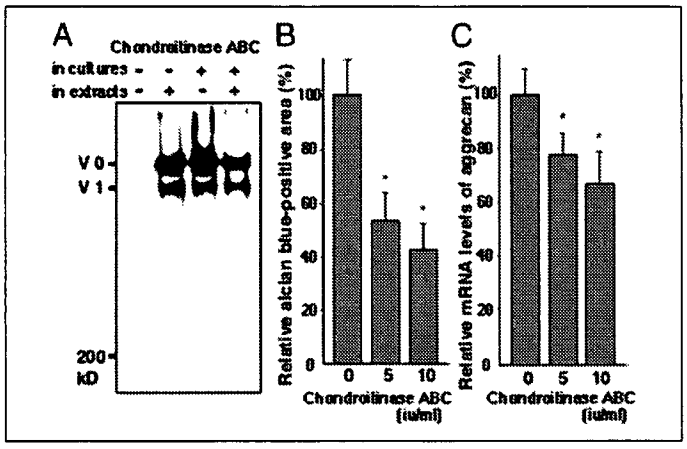

FIGURE 5. **Involvement of the chondroitin sulfate chains in the chondrogenesis.** *A*, immunoblotting for versican/PG-M core bands on SDS-PAGE of the extracts of the N1511 cells. The cells were first treated in cultures with 5 units/ml chondroitinase ABC, and the cell extracts were then exposed with or without chondroitinase ABC to confirm that the chondroitin sulfate chains of versican/PG-M were well digested in the culture media. Note that the core bands from the cells treated only "in cultures" are similar to those treated only "in extracts," in comparison with the sample with both treatments of in cultures and in extracts, and also with negative control (no treatment). *B*, effects of the treatment with chondroitinase ABC in the early phase of the cultures (day 0–4) at different concentrations on the chondrogenic differentiation were shown by the relative Alcian blue-positive area (per well) at day 18. *C*, the effects of the treatment were also shown by the relative transcriptional levels of aggrecan at day 13, which were measured by quantitative real time PCR. Values in *B* and *C* were the means ± S.D. ($n = 50$ for *B* and $n = 9$ for *C*), and the *asterisks* indicated a significant difference from control (0 IU/ml) (Student's *t* test; *, $p < 0.01$).

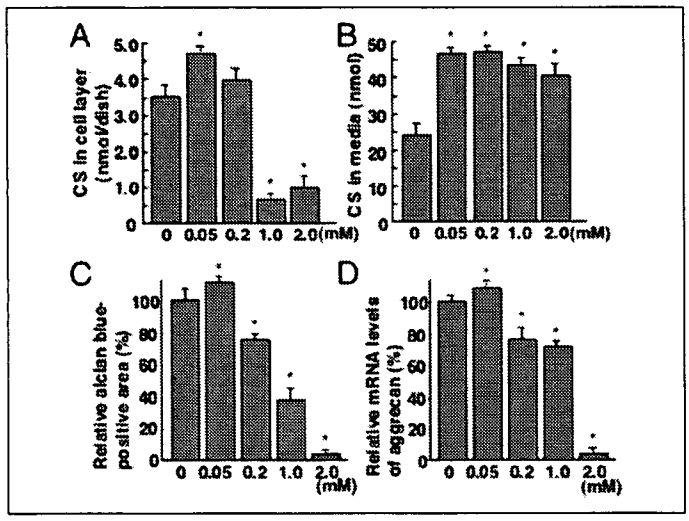

FIGURE 6. **Effects of the treatment with β-xyloside on chondrogenesis.** Induced N1511 cells were treated with β-xyloside at various concentrations indicated during the early phase of chondrogenesis (day 0–5). The amounts of chondroitin sulfates (*CS*) in cell layers at day 5 (*A*) and in combined culture media from day 1 to 5 (*B*) were measured by chromatography as described under "Experimental Procedures." Less CS was detected at the concentration over 1.0 mM in cell layers, and more CS was in media at all the concentrations other than nontreatment (0 mM). *C*, Alcian blue-positive area in cultures at day 18 was quantified as described under "Experimental Procedures." *D*, transcriptional levels of aggrecan were analyzed by quantitative real time PCR at day 13. Results were normalized using the GAPDH transcription levels. Values in *A–D* were the mean ± S.D. obtained from three independent experiments performed in triplicate ($n = 9$ for *A*, *B* and *D*; $n = 50$ for *C*). The *asterisks* indicated a significant difference from control (0 mM) (Student's *t* test; *, $p < 0.01$).

concentration over 1.0 mM, the cells morphologically changed to be fibroblast-like phenotypes at day 2 (data not shown), and Alcian blue-positive areas were reduced dose-dependently at the concentrations over 0.2 mM at day 18 (Fig. 6*C*). Also, transcription of aggrecan synthesis was suppressed at the concentration over 0.2 mM (Fig. 6*D*). α-Xyloside

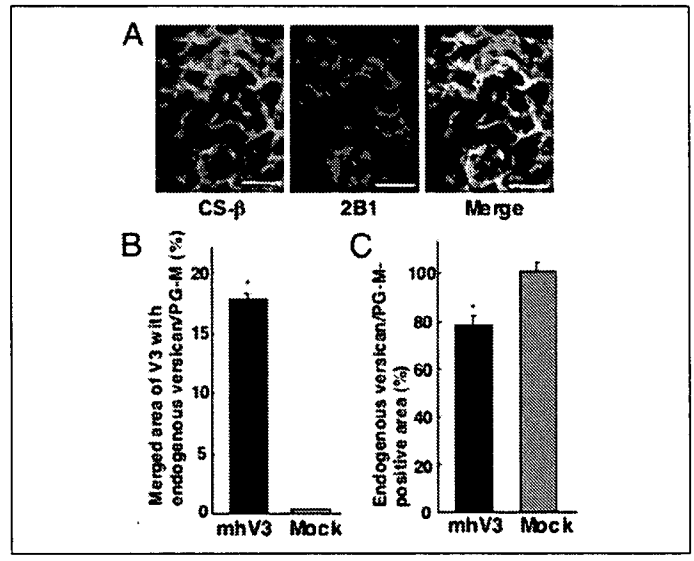

FIGURE 7. **Effects of abnormal expression of V3 on the distribution of endogenous versican/PG-M in the ECM.** Mouse V3 with a human-specific epitope of 2B1 (mhV3) was transiently overexpressed at day 2. *A*, the distribution of mhV3 (see the 2B1-stained red fluorescence, *middle*) was similar to that of the endogenous versican/PG-M (see the CS-β-stained green fluorescence, *left*) in the ECM, but some areas had only V3 (see the merged pattern, *right*). *Bars*, 100 mm. *B*, statistical measurement revealed that in mhV3-transfected culture (*mhV3*) the merged area (*yellow* fluorescent pattern, *right panel* in *A*) was 17% of endogenous forms of versican/PG-M (*green* fluorescent pattern, *left panel* in *A*), whereas there was no merged area in mock vector-transfected cultures (*Mock*). *C*, statistical measurement also revealed that there was less deposition of endogenous forms of versican/PG-M in mhV3-transfected cultures (*mhV3*), compared with mock vector-transfected cultures (*Mock*). Values in *B* and *C* represented the mean ± S.D. ($n = 50$) from three independent experiments performed in triplicate. A significant difference from Mock was indicated by the *asterisk* in *B* and *C* (Student's *t* test; *, $p < 0.001$).

did not show significant effect (data not shown). β-Xyloside appeared to disrupt mesenchymal cell condensation phenotype through the alternation of CS synthesis and to inhibit chondrogenesis. These results suggested that the chondroitin sulfate portions of versican/PG-M contribute to the early phase of the chondrocyte differentiation.

Alteration of the Extracellular Matrix in the Early Phase of Chondrogenesis by Overexpression of the V3 Form—We also hypothesized that irregular expression of the V3 form of versican/PG-M, a spliced variant lacking the chondroitin sulfate-attachment domains, may suppress the deposition of V0 and V1 forms in the matrix in a competitive manner because of the sharing of the G1 and G3 domain binding functions with endogenous forms, which would have resulted in inhibition of the mesenchymal cell condensation-like process by the reduction of chondroitin sulfate chains in the matrix. We transiently transfected N1511 cells with the cDNA for mouse V3 with a human-specific epitope of 2B1 so that the expression of V3 coincided with that of native versican/PG-M forms (V0 and V1), and also the localization of V3 and endogenous versican/PG-M was individually visualized by immunostaining of cultures with the 2B1 monoclonal antibody and anti-mouse CS-β antibodies, respectively. At day 2, about 17% of endogenous versican/PG-M in the ECM was colocalized with overexpressed V3 (Fig. 7, *A* and *B*), and some area only had V3. When V3 was deposited in the ECM, less endogenous versican/PG-M was deposited in the ECM than in a mock-transfected culture (Fig. 7*C*). The expression levels of the native forms (V0 and V1) in the early phase were not affected by the transcription of V3 because they were the same as the ones of the mock-transfected cells in the RT-PCR analysis (Fig. 8*A*). In addition, the quantitative RT-PCR demonstrated that relative mRNA levels of the native forms (V0 + V1) did not differ between V3- and mock-transfected cells (Fig. 8*B*). The distribution of other ECM molecules such as hyalauronan and fibronectin, which have been shown to bind to the G1 domain of versican/PG-M

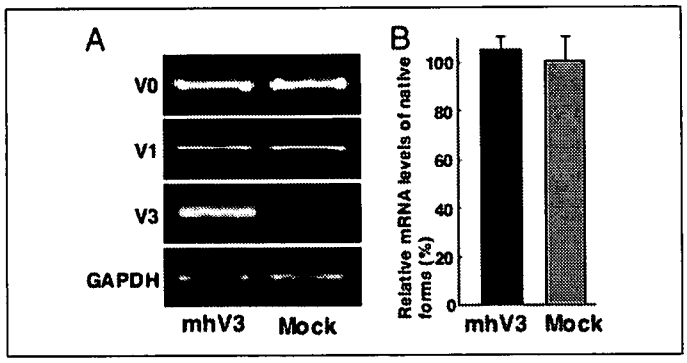

FIGURE 8. **No alteration of endogenous versican/PG-M expression in the cells abnormally expressing V3.** *A*, RT-PCR analysis shows that expression patterns of native forms of versican/PG-M (V0 and V1) were not altered in the 1-day culture of mhV3-tranfected cells (*mhV3*). *B*, quantitative real time PCR for endogenous versican/PG-M gene expression in the above culture revealed no significant difference of the expression level between the cells abnormally expressing V3 (*mhV3*) and mock-transfectants (*Mock*). Values were normalized using the GAPDH transcriptional levels and were the means ± S.D. from three independent experiments in triplicate ($n = 9$).

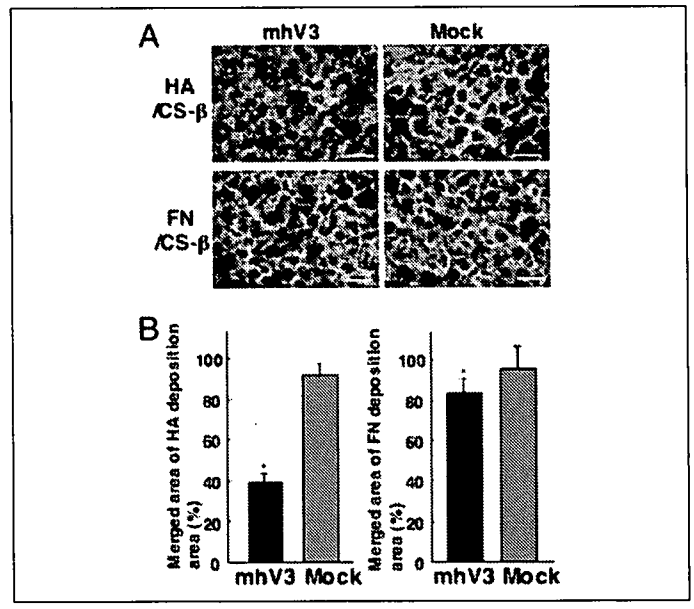

FIGURE 9. **Alteration of the distributions of endogenous versican/PG-M and other molecules in the ECM with the abnormal expression of V3.** *A*, the mhV3- and mock-transfected cells at day 2 were doubly stained for hyaluronan and endogenous versican/PG-M (*HA/CS-β*) or for fibronectin and endogenous versican/PG-M (*FN/CS-β*), respectively. The distribution of hyaluronan or fibronectin and endogenous versican/PG-M (CS-β) differed between mhV3- and mock-transfected cell cultures. *Bars*, 100 μm. *B*, the merged area of native hyalauronan (*HA*) or fibronectin (*FN*) with endogenous versican/PG-M (HA/CS-β) was quantified as described under "Experimental Procedures," which revealed the reduction of the areas in antisense-transfected cultures (*mhV3*). Values in *B*, *left* and *right panels*, represented the mean ± S.D. ($n = 50$) from three independent experiments in triplicate. A significant difference from Mock was indicated by the *asterisks* (Student's *t* test; *, $p < 0.01$).

(31), was altered because endogenous versican/PG-M (stained with Texas Red) showed less overlap in its deposition with hyaluronan (stained with FITC) and fibronectin (stained with FITC) compared with mock transfectants on day 2 (Fig. 9*A*). Statistical analysis for the merged area of native HA or FN showed that both the areas were reduced in antisense-transfected cultures (Fig. 9*B*). These results suggest that abnormal expression of the V3 form affected the formation of ECM suitable for the early phase of chondrogenesis.

Suppression of Chondrogenesis by Overexpression of V3—We examined the effect of the overexpression of V3 on the chondrocyte differentiation. The V3-transfected cell culture at day 13 showed decreased Alcian blue staining of the ECM, compared with the mock-transfected cell culture (Fig. 10*A*). Statistical analysis also confirmed this reduction (Fig. 10*B*). In the V3-transfected cells, the deposition of aggrecan decreased where the V3 form was overexpressed at day 13 (Fig. 10*C*). Most of the aggrecan staining in V3-overexpressing cells was observed where V3 was not deposited. It is of note that the deposition of aggrecan in both the cultures was observed, where endogenous versican/PG-M had been heavily deposited as shown in Fig. 2*C* (data not shown). Furthermore, where the V3 form was overexpressed at day 13 in the V3-transfected cells, the deposition of native forms (V0/V1) decreased as shown in Fig. 7*C* (data not shown), and the aggrecan transcription level was decreased to one-fourth, compared with the mock-transfected cells at day 13 (Fig. 10*D*). The results suggest that the abnormal expression of the V3 form comprising only the G1 and G3 domains without any of the chondroitin sulfate-attachment domains interrupted the normal function of the wild type forms of versican/PG-M by decreasing the deposition in the ECM and suppressed the chondrocyte differentiation at the transcriptional level. This finding also suggested that the V0/V1 forms play a pivotal role in the chondrocytic differentiation of N1511 cells.

Considering the fact that the V3 form differs from the V0 and V1 forms in terms of the absence of the chondroitin sulfate-attachment domains as well as the negative effects of both β-xyloside and chondroitinase ABC treatments on the chondrogenesis, it is likely that versican/PG-M with chondroitin sulfate chains in mesenchymal ECM plays a crucial role in positively regulating mesenchymal cell condensation and subsequent chondrogenesis *in vitro*.

DISCUSSION

In this study, we have demonstrated for the first time that a marked expression and deposition of versican/PG-M in the mesenchymal ECM are required for subsequent chondrocytic gene expression. The V0 and V1 forms of versican/PG-M are important for this activity, and their chondroitin sulfate chains are the crucial molecular portions. The evidence is as follows. 1) The correlation between early expression of versican/PG-M and later chondrogenesis, shown in Fig. 1 suggests that a transiently high expression of V0/V1 forms of versican/PG-M always precedes aggrecan expression at both the mRNA and protein levels. 2) The inhibition of versican/PG-M synthesis and deposition by the expression of antisense RNA caused suppressed or no gene expression, synthesis, and deposition of aggrecan. 3) When the chondroitin sulfate chains mainly in V0/V1 forms of versican/PG-M were degraded in the ECM by treatment with chondroitinase ABC, the aggrecan mRNA levels as well as the accumulation in the ECM were largely suppressed. 4) The reduction of chondroitin sulfate chains by β-xyloside treatment inhibited the deposition of mesenchymal ECM and suppressed the expression of aggrecan mRNA. 5) When the V3 form that has no chondroitin sulfate-attachment domain was forced to express, it caused significant changes in the organization of the mesenchymal ECM and consequently suppressed the chondrocyte differentiation. The cells only exhibited the accumulation of aggrecan in the area of ECM where there was no V3 deposition.

The expression patterns of versican/PG-M and aggrecan in N1511 mimic quite well the *in vivo* mesenchymal condensation and subsequent chondrogenesis, that is the high level of expression and the deposition in the ECM of versican/PG-M and the subsequent gradual attenuation proceeded by the accumulation of aggrecan in the ECM (10, 22–24). The N1511 cells are induced to become chondrocytes not only by treatment with PTH and dexamethasone in the presence of serum but also by that of BMP-2 and insulin in the absence of serum. When exposed to BMP-2/insulin, N1511 cells show Col10α1 expression and undergo further steps of chondrocyte differentiation toward hypertro-

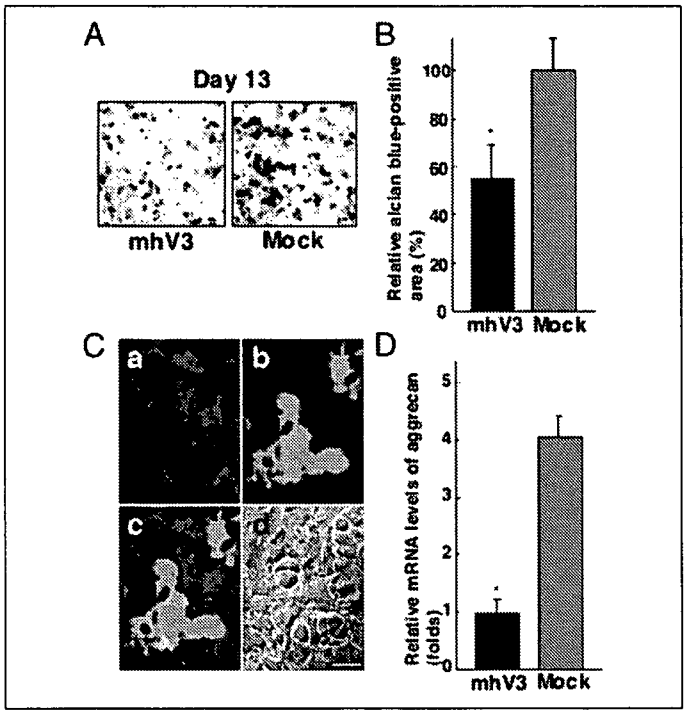

FIGURE 10. **Suppression of chondrogenesis by the abnormal expression of V3.** The V3-transfected cells (*mhV3*) at day 13 showed a reduction in the Alcian blue-positive area of up to 55% in comparison with mock-transfected cells (*Mock*). *A*, an example for the Alcian blue staining. *B*, quantification of the positive areas. Values were obtained from three separate experiments performed in triplicate (mean ± S.D., $n = 50$, $p < 0.01$ with Student's *t* test). *Bars*, 100 μm. *C*, double staining of the V3-transfected cells at day 13 for V3 (*red* fluorescence in *panel a*) and aggrecan (*green* fluorescence in *panel b*). Where V3 was not deposited, the accumulation of aggrecan was observed (see the merged pattern *panel c*). *Panel d*, phase contrast. *D*, the transcriptional levels of aggrecan in V3-transfected cells (*mhV3*) at day 13 were compared with those in mock-transfected cells (*Mock*), and the levels were less than one-fourth. Values in *B* and *D* were obtained by three independent experiments in triplicate (mean ± S.D., $n = 50$ in *B* and $n = 9$ in *D*). A significant difference from Mock was indicated by the *asterisks* in *B* and *D* (Student's *t* test; *, $p < 0.01$).

phy and mineralization, *i.e.* terminal differentiation (38). Versican/PG-M has also been shown to be strongly expressed in the ECM in the early phase of chondrocyte differentiation, when induced by BMP-2 and insulin (date not shown). N1511 cells have already expressed a low level of Sox9 without the induction of type II collagen and aggrecan gene expression (data not shown), and the cells appear to be in the differentiation phase committed to chondrogenesis, in comparison with other multipotential cell lines such as C3H10T1/2 and C1. In addition, N1511 cells expressed a type IIA procollagen mRNA at day 0, which is known to be preferentially expressed in prechondrocytes/chondroblasts (48). N1511 cells also expressed a PTH/PTHrP receptor, a critical regulator of chondrocyte proliferation and differentiation (49–51), whereas undifferentiated and early stage ATDC5 cells lack a PTH/PTHrP receptor (52), and PTH treatment fails to up-regulate the proliferation of ATDC5 cells (53, 54). Therefore, to our knowledge, the system using N1511 cells treated with PTH and dexamethasone may be the best *in vitro* system available for analyzing the role of versican/PG-M in the early phases of chondrocyte differentiation (mesenchymal cell condensation step).

N1511 cells in the early phases of the differentiation express N-cadherin, neural cell adhesion molecule, hyaluronan, type I collagen, tenasin, and fibronectin (data not shown and Fig. 9*A*), of which the former two molecules are known to be involved in mesenchymal cell-cell interactions (6, 7, 55), and the latter molecules are known to be typical ECM components during mesenchymal cell condensation and interact with versican/PG-M directly to form the mesenchymal ECM (28). Moreover, the expression of the versican/PG-M gene (*Cspg2*) is regulated by a promoter that includes a LEF-binding site, which is one of the targets of N-cadherin (25). N-cadherin, a cell-cell interaction molecule expressed in the mesenchymal cell condensation area has been shown to be involved in chondrogenesis (6, 55, 56). It has also been shown that N-cadherin-mediated cell adhesion is suppressed by activation of a so-called repulsive receptor, Roundabout (Robo), by the binding of its ligand, Slit (57). However, there is no evidence that versican/PG-M is involved in this Slit-Robo interaction.

The suppression of chondrogenesis of N1511 by the antisense expression for versican/PG-M and by forced expression of the variant V3 correlated well with the inhibition of the deposition and the abnormal organization of versican/PG-M in the ECM. Although the results could be explained simply by the possibility that the suppressed or abnormal deposition of endogenous versican/PG-M prevents aggrecan from binding with hyaluronan, real time quantitative RT-PCR has revealed that both the antisense expression for versican/PG-M and the forced expression of the V3 form caused a low level of aggrecan mRNA (Fig. 3*D* and Fig. 10*D*), indicating that versican/PG-M deposited in the ECM at the early phase of the differentiation signals the cells and regulates the gene transcription. In addition, our findings have revealed that the chondroitin sulfate chain portions of versican/PG-M may play a pivotal role. Four variants of versican/PG-M (V0, V1, V2, and V3) have different amounts and numbers of chondroitin sulfate chains (16). It is interesting that V0 (G1-CS-α-CS-β-G3) and V1 (G1-CS-β-G3) are expressed in the heart and blood vessels where cell shapes are thought to be actively changed, whereas V2 (G1-CS-α-G3) is mainly expressed in brain where the cell shape appears to be stable. In N1511 cells, early in the chondrocyte differentiation, V0 and V1 forms were expressed, and the V2 form was not expressed until late. It is also interesting that mesenchymal cell condensation largely involves changes in cell shape, whereas differentiated chondrocytes are thought to have a rather stable shape. It is also important to clarify the mechanism by which the variant form changes in a tissue- and differentiation stage-dependent manner, but this has not yet been studied.

The V3 form, composed of only G1 and G3 domains, has not been detected *in vivo*, but overexpressed V3 actually deposited in the ECM and partially colocalized with endogenous versican/PG-M. Our finding that overexpressed V3 inhibited chondrogenesis is in line with the observation that the exogenous addition of the G3 domain of versican/PG-M to culture medium inhibited the chondrogenesis of mesenchymal cells (58), because the added G3 domain may have occupied sites on the mesenchymal ECM for the versican/PG-M binding, interrupted deposition of native versican/PG-M, and resulted in a significant alteration of matrix function. Moreover, there is a report that retrovirally mediated overexpression of the V3 form showed opposite effects to other variants of versican/PG-M in terms of cell adhesion, migration, and proliferation in arterial smooth muscle cells, *i.e.* the cells expressing V3 spread more on tissue culture dishes with larger areas of close and focal contacts, grew slower, and migrated a shorter distance than control cells (59).

The V3 form is more than 1000 amino acids shorter than V2 and V1 (Fig. 4*A*). Therefore, one possibility still remains that this significant amount of protein could have some biological effects on the ECM, resulting in inhibition of chondrogenesis. But results obtained from the β-xyloside treatment in cultures led us to think that this possibility is less likely than our hypothesis, because β-xyloside is known to affect directly and specifically the normal chondroitin sulfate chain synthesis on the core proteins. Besides, β-xyloside also yielded core protein-free chondroitin sulfate with short and undersulfated chains, and then nor-

mal collagen synthesis is inhibited (42, 60). It is interesting to see that temporal and significant stimulation of chondrogenesis was observed at the low concentration of β-xyloside (0.05 mM; Fig. 6, *C* and *D*) and well correlated with the increase of chondroitin sulfates in cell layers (0.05 mM; Fig. 6*A*). Because we showed previously that β-xyloside at such low concentrations yielded xyloside-derivatized chondroitin sulfate chains with the size and sulfation degree similar to the native ones (47), it is likely that the increased chondroitin sulfates in cell layers may be xyloside-derivatized chains.

Taken together, we could conclude that versican/PG-M with chondroitin sulfate chains is crucial for positively regulating mesenchymal condensation and subsequent chondrocyte differentiation. Moreover, we may hypothesize that chondroitin sulfate chains of versican/PG-M deposited in the mesenchymal ECM interact with cells via specific cell surface receptors or by providing cells with some physical environment suitable for migration and/or controlling cell shape, if they are active agents in induction of chondrogenesis. Although definite and convincing evidence for the receptor(s) for the chondroitin sulfate chains has not been available so far, there are a few candidates such as annexin VI and midkine that bind to the CS chains of versican/PG-M on the cell surface *in vitro* (33, 61). Annexin VI has been shown to interact with the chondroitin sulfate chains in the ECM and to inhibit the subsequent cell spreading, although the mechanism is totally unknown (33). The chondroitin sulfate chains may be involved in mesenchymal condensation and further chondrogenesis by modifying cell-extracellular matrix molecule interactions so as to influence the cell shape.

Versican/PG-M-deficient mice died at embryonic day 10.5, because of a heart problem before the onset of chondrogenesis (37). This abnormality was caused by a defect in the transformation of the endothelium into the mesenchyme because of irregular cell migration and adhesion. This result is consistent with our finding that versican/PG-M can suppress interactions between cells and most ECM molecules such as fibronectin through the chondroitin sulfate chains (30–32). Also, antiadhesive function of versican/PG-M may be affected by the treatment with β-xyloside in culture, because the morphological changes of cells are consistent with our previous data (30). To elucidate the function of versican/PG-M during chondrogenesis as well as organogenesis in which mesenchymal condensation is involved, studies with conditional knock-out mice and transgenic mice with tissue-specific or stage-specific expression may be necessary. Moreover, the relationships among cell-matrix interaction molecules, versican/PG-M, and cell-cell interaction molecules should be studied further, which may provide some idea as to the mechanism of action of versican/PG-M in chondrogenesis.

Acknowledgments—We are grateful to Drs. A. Jikko and C. Damsky for their generous support and useful discussions. We are also grateful to Drs. M. Zako and K. Ito for the construction of the vectors of versican/PG-M variant forms. We also thank Dr. Mishina for his generous reading of the manuscript.

REFERENCES

1. Fell, H. B. (1925) *J. Morphol.* **40,** 417–451
2. Jurand, A. (1965) *Proc. R. Soc. Lond.* **162,** 387–405
3. Leonard, C. M., Fuld, H. M., Frenz, D. A., Downie, S. A., Massague, J., and Newman, S. A. (1991) *Dev. Biol.* **145,** 99–109
4. Storm, E. E., Huynh, T. V., Copeland, N. G., Jenkins, N. A., Kingsley, D. M., and Lee, S. J. (1994) *Nature* **368,** 639–643
5. Blessing, M., Nanney, L. B., King, L. E., Jones, C. M., and Hogan, B. L. (1993) *Genes Dev.* **7,** 204–215
6. Oberlender, S. A., and Tuan, R. S. (1994) *Development (Camb.)* **120,** 177–187
7. Widelitz, R. B., Jiang, T. X., Murray, B. A., and Chuong, C. M. (1993) *J. Cell. Physiol.* **156,** 399–411
8. Frenz, D. A., Jaikaria, N. S., and Newman, S. A. (1989) *Dev. Biol.* **136,** 97–103
9. Mackie, E. J., Thesleff, I., and Chiquet-Ehrismann, R. (1987) *J. Cell Biol.* **105,** 2569–2579
10. Kimata, K., Oike, Y., Tani, K., Shinomura, T., Yamagata, M., Uritani, M., and Suzuki, S. (1986) *J. Biol. Chem.* **261,** 13517–13525
11. Maleski, M. P., and Knudson, C. B. (1996) *Exp. Cell Res.* **225,** 55–66
12. Gould, S. E., Upholt, W. B., and Kosher, R. A. (1992) *Proc. Natl. Acad. Sci. U. S. A.* **89,** 3271–3275
13. French, M. M., Smith, S. E., Akanbi, K., Sanford, T., Hecht, J., Farach-Carson, M. C., and Carson, D. D. (1999) *J. Cell Biol.* **145,** 1103–1115
14. Zimmermann, D. R., and Ruoslahti, E. (1989) *EMBO J.* **8,** 2975–2981
15. Ito, K., Shinomura, T., Zako, M., Ujita, M., and Kimata, K. (1995) *J. Biol. Chem.* **270,** 958–965
16. Shinomura, T., Zako, M., Ito, K., Ujita, M., and Kimata, K. (1995) *J. Biol. Chem.* **270,** 10328–10333
17. LeBaron, R. G., Zimmermann, D. R., and Ruoslahti, E. (1992) *J. Biol. Chem.* **267,** 10003–10010
18. Ujita, M., Shinomura, T., Ito, K., Kitagawa, Y., and Kimata, K. (1994) *J. Biol. Chem.* **269,** 27603–27609
19. Shinomura, T., Nishida, Y., Ito, K., and Kimata, K. (1993) *J. Biol. Chem.* **268,** 14461–14469
20. Zako, M., Shinomura, T., Ujita, M., Ito, K., and Kimata, K. (1995) *J. Biol. Chem.* **270,** 3914–3918
21. Dours-Zimmermann, M. T., and Zimmermann, D. R. (1994) *J. Biol. Chem.* **269,** 32992–32998
22. Shinomura, T., Jensen, K. L., Yamagata, M., Kimata, K., and Solursh, M. (1990) *Anat. Embryol.* **181,** 227–233
23. Yamagata, M., Shinomura, T., and Kimata, K. (1993) *Anat. Embryol.* **187,** 433–444
24. Shibata, S. F. K., Imai, H., Abe, T., and Yamashita, Y. (2003) *J. Anat.* **203,** 425–432
25. Kishimoto, J., Ehama, R., Wu, L., Jiang, S., Jiang, N., and Burgeson, R. E. (1999) *Proc. Natl. Acad. Sci. U. S. A.* **96,** 7336–7341
26. Henderson, D. J., and Copp, A. J. (1998) *Circ. Res.* **83,** 523–532
27. Steer, D. L., Shah, M. M., Bush, K. T., Stuart, R. O., Sampogna, R. V., Meyer, T. N., Schwesinger, C., Bai, X., Esko, J. D., and Nigam, S. K. (2004) *Dev. Biol.* **272,** 310–327
28. Yamagata, M., Yamada, K. M., Yoneda, M., Suzuki, S., and Kimata, K. (1986) *J. Biol. Chem.* **261,** 13526–13535
29. Matsumoto, K. S. M., Go, M., Shimizu, K., Shinomura, T., Kimata, K., and Watanabe, H. (2003) *J. Biol. Chem.* **278,** 41205–41212
30. Yamagata, M., Suzuki, S., Akiyama, S. K., Yamada, K. M., and Kimata, K. (1989) *J. Biol. Chem.* **264,** 8012–8018
31. Yamagata, M., Saga, S., Kato, M., Bernfield, M., and Kimata, K. (1993) *J. Cell Sci.* **106,** 55–65
32. Yamagata, M., and Kimata, K. (1994) *J. Cell Sci.* **107,** 2581–2590
33. Takagi, H., Asano, Y., Yamakawa, N., Matsumoto, I., and Kimata, K. (2002) *J. Cell Sci.* **115,** 3309–3318
34. Shinomura, T., Nshida, Y., and Kimata, K. (1991) in *Articular Cartilage and Osteoarthritis* (Kuettner, K. E., Schleyerbach, R., Peyron, J. G., and Hascall, V. C., eds) pp. 35–44, Raven Press, Ltd., New York
35. Solursh, M., Jensen, K. L., Zanetti, N. C., Linsenmayer, T. F., and Reiter, R. S. (1984) *Dev. Biol.* **105,** 451–457
36. Zhang, Y. W. Y., Cao, L., Lee, V., Chen, L., Lin, Z., Kiani, C., Adams, M. E., and Yang, B. B. (2001) *Exp. Cell Res.* **263,** 33–42
37. Mjaatvedt, C. H., Yamamura, H., Capehart, A. A., Turner, D., and Markwald, R. R. (1998) *Dev. Biol.* **202,** 56–66
38. Kamiya, N., Jikko, A., Kimata, K., Damsky, C., Shimizu, K., and Watanabe, H. (2002) *J. Bone Miner. Res.* **17,** 1832–1842
39. Sobue, M., Nakashima, N., Fukatsu, T., Nagasaka, T., Fukata, S., Ohiwa, N., Nara, Y., Ogura, T., Katoh, T., and Takeuchi, J. (1989) *Histochem. J.* **21,** 455–460
40. Itano, N., Atsumi, F., Sawai, T., Yamada, Y., Miyaishi, O., Senga, T., Hamaguchi, M., and Kimata, K. (2002) *Proc. Natl. Acad. Sci. U. S. A.* **99,** 3609–3614
41. Oike, Y., Kimata, K., Shinomura, T., Nakazawa, K., and Suzuki, S. (1980) *Biochem. J.* **191,** 193–207
42. Sobue, M., Habuchi, H., Ito, K., Yonekura, H., Oguri, K., Sakurai, K., Kamohara, S., Ueno, Y., Noyori, R., and Suzuki, S. (1987) *Biochem. J.* **241,** 591–601
43. Nogami, K., Suzuki, H., Habuchi, H., Ishiguro, N., Iwata, H., and Kimata, K. (2004) *J. Biol. Chem.* **279,** 8219–8229
44. Isogai, Z., Shinomura, T., Yamakawa, N., Takeuchi, J., Tsuji, T., Heinegard, D., and Kimata, K. (1996) *Cancer Res.* **56,** 3902–3908
45. Watanabe, H., de Caestecker, M. P., and Yamada, Y. (2001) *J. Biol. Chem.* **276,** 14466–14473
46. Zako, M., Shinomura, T., and Kimata, K. (1997) *J. Biol. Chem.* **272,** 9325–9331
47. Kato, Y., Kimata, K., Ito, K., Karasawa, K., and Suzuki, S. (1978) *J. Biol. Chem.* **253,** 2784–2789
48. Sandell, L. J., Nalin, A. M., and Reife, R. A. (1994) *Dev. Dyn.* **199,** 129–140
49. Lanske, B., Karaplis, A. C., Lee, K., Luz, A., Vortkamp, A., Pirro, A., Karperien, M.,

Defize, L. H., Ho, C., Mulligan, R. C., Abou-Samra, A. B., Juppner, H., Segre, G. V., and Kronenberg, H. M. (1996) *Science* **273,** 663–666
50. Amizuka, N., Warshawsky, H., Henderson, J. E., Goltzman, D., and Karaplis, A. C. (1994) *J. Cell Biol.* **126,** 1611–1623
51. Goltzman, D. (1999) *J. Bone Miner. Res.* **14,** 173–177
52. Shukunami, C., Shigeno, C., Atsumi, T., Ishizeki, K., Suzuki, F., and Hiraki, Y. (1996) *J. Cell Biol.* **133,** 457–468
53. Shukunami, C., Ohta, Y., Sakuda, M., and Hiraki, Y. (1998) *Exp. Cell Res.* **241,** 1–11
54. Shukunami, C., Ishizeki, K., Atsumi, T., Ohta, Y., Suzuki, F., and Hiraki, Y. (1997) *J. Bone Miner. Res.* **12,** 1174–1188
55. Chimal-Monroy, J., and de León, L. D. (1999) *Int. J. Dev. Biol.* **43,** 59–67
56. Tufan, A. C., Daumer, K. M., DeLise, A. M., and Tuan, R. S. (2002) *Exp. Cell Res.* **273,** 197–203
57. Rhee, J., Mahfooz, N. S., Arregui, C., Lilien, J., Balsamo, J., and Van Berkum, M. F. A. (2002) *Nat. Cell Biol.* **4,** 798–805
58. Zhang, Y., Cao, L., Kiani, C. G., Yang, B. L., and Yang, B. B. (1998) *J. Biol. Chem.* **273,** 33054–33063
59. Lemire, J. M., Merrilees, M. J., Braun, K. R., and Wight, T. N. (2002) *J. Cell. Physiol.* **190,** 38–45
60. Gibson, K. D., Segen, B. J., and Audhya, T. K. (1977) *Biochem. J.* **162,** 217–233
61. Zou, K., Muramatsu, H., Ikematsu, S., Sakuma, S., Salama, R. H., Shinomura, T., Kimata, K., and Muramatsu, T. (2000) *Eur. J. Biochem.* **267,** 4046–4053

THE JOURNAL OF BIOLOGICAL CHEMISTRY VOL. 281, NO. 26, pp. 18257–18263, June 30, 2006
Printed in the U.S.A.

Identification and Characterization of Versican/PG-M Aggregates in Cartilage*

Received for publication, September 20, 2005, and in revised form, April 26, 2006 Published, JBC Papers in Press, April 28, 2006, DOI 10.1074/jbc.M510330200

Kazu Matsumoto[‡§], Nobuhiro Kamiya[‡§], Keittisak Suwan[‡], Fukiko Atsumi[‡], Katsuji Shimizu[§], Tamayuki Shinomura[‡¶], Yoshihiko Yamada[‖], Koji Kimata[‡], and Hideto Watanabe[‡1]

From the [‡]Institute for Molecular Science of Medicine, Aichi Medical University, Nagakute, Aichi 480-1195, Japan, [§]Department of Orthopaedic Surgery, Gifu University School of Medicine, Gifu 500-8705, Japan, [¶]Tissue Regeneration, Department of Hard Tissue Engineering, Tokyo Medical and Dental University, Tokyo 113-8549, Japan, and [‖]Craniofacial Developmental Biology and Regeneration Branch, NIDCR, National Institutes of Health, Bethesda, Maryland 20892-4370

Versican/PG-M is a large chondroitin sulfate proteoglycan of the extracellular matrix with a common domain structure to aggrecan and is present in cartilage at low levels. Here, we characterized cartilage versican during development and growth. Immunostaining showed that versican was mainly localized in the interterritorial zone of the articular surface at 2 weeks in mice, whereas aggrecan was in the pericellular zone of prehypertrophic and hypertrophic cells of the growth plate. Although its transcription level rapidly diminished during growth, versican remained in the articular cartilage. Biochemical analysis of normal articular cartilage and aggrecan-null cartilage from cmd (cartilage matrix deficiency)/cmd mice revealed that versican was present as a proteoglycan aggregate with both link protein and hyaluronan. Chondroitin sulfate chains of versican digested with chondroitinase ABC contained 71% nonsulfated and 28% 4-sulfated unsaturated disaccharides, whereas those of aggrecan contained 25% nonsulfated and 70% 4-sulfated. Link protein overexpression in chondrocytic N1511 cells at the early stage of differentiation, in which versican is expressed, enhanced versican deposition in the matrix and prevented subsequent aggrecan deposition. These results suggest that versican is present as an aggregate distinct from the aggrecan aggregate and may play specific roles in the articular surface.

Versican/PG-M (1, 2) is a large chondroitin sulfate proteoglycan of the extracellular matrix (ECM)[2] that exhibits two distinct expression patterns. In various developing embryonic tissues (3), including the nervous system, versican is transiently expressed and plays important roles in cell adhesion (4), migration (5), proliferation, and differentiation (6). In some adult tissues, such as the heart, blood vessels, and brain, it is constitutively expressed and serves as a structural macromolecule of the ECM.

In developing cartilage, versican is transiently expressed at a high level in the mesenchymal condensation area and rapidly disappears during cartilage development (7, 8). Recent immunohistochemical studies on developing limb bud cartilage revealed that an area positive for versican gradually shifts out of the diaphysis and is replaced by an area positive for aggrecan. Differentiating chondrocytic N1511 and ATDC5 cells showed similar expression patterns of these molecules (9). These reciprocal patterns of versican and aggrecan expression suggest that versican serves as a temporary framework in developing cartilage matrix. Although the aggrecan aggregate (10) is the major component of cartilage ECM and versican has not been detected by immunohistochemical studies (3), constitutive low level transcription of the versican gene is observed in cartilage (11) and chondrocytes (11, 12). In addition, extracts of human adult articular cartilage contain versican (13), suggesting its distinct role there.

The core protein of versican consists of N- and C-terminal globular domains (G1 and G3) and two chondroitin sulfate (CS) domains (CS-α and CS-β). The N-terminal G1 comprises A, B, and B′ loops and binds to both hyaluronan (HA) (14) and link protein (LP). The C-terminal G3 domain binds fibulin-1 and -2 (15, 16), tenascins (17, 18), and heparan sulfate proteoglycans (19). As aggrecan in cartilage forms a proteoglycan aggregate with both HA and LP, versican is believed to form similar stable aggregates in the presence of both HA and LP. Indeed, versican aggregates have been isolated from dental pulp (8), and versican secreted from cultured vascular smooth muscle cells forms aggregates with HA and LP (20).

We recently demonstrated that the versican G1 domain binds to both LP and HA in a different manner than aggrecan G1 (21); the B-B′ segments of LP and versican G1 bind each other, whereas the A loops of LP and aggrecan G1 interact. These results suggest that versican is present as an aggregate in articular cartilage, with HA and LP, and plays a unique role distinct from the aggrecan aggregate. However, the versican aggregate has not been identified in cartilage, and the function of versican has not been determined.

In this study, we investigated the expression, localization, and aggregate formation of versican in cartilage to gain insights into its function. Versican was mainly localized in the interterritorial zone of the articular surface, whereas aggrecan was rather diffused, especially with dense staining in the territorial zone of prehypertrophic chondrocytes. The versican aggregate was isolated by cesium chloride density gradient ultracentrifugation from normal articular and aggrecan-null cartilage. Although transcription of the versican gene dramatically decreased after birth, versican remained in the articular cartilage in the form of the proteoglycan aggregate. LP overexpression in chondrocytic N1511 cells, which synthesize versican at the early stage of differentiation, significantly enhanced versican deposition and inhibited subsequent aggrecan deposition. These results suggest that the versican aggregate is present in the articular surface and may provide ECM properties distinct from deeper zones where aggrecan aggregates are abundant.

* This work was supported by a grant-in-aid for scientific research on priority areas (KAKENHI to H. W.) and a grant-in-aid for scientific research (KAKENHI to H. W.). The costs of publication of this article were defrayed in part by the payment of page charges. This article must therefore be hereby marked "*advertisement*" in accordance with 18 U.S.C. Section 1734 solely to indicate this fact.

[1] To whom correspondence should be addressed: Inst. for Molecular Science of Medicine, Aichi Medical University, Karimata 21, Yazako, Nagakute, Aichi-gun, Aichi 480-1195, Japan. Tel.: 81-561-62-3311 (ext. 2086); Fax: 81-561-63-3532; E-mail: wannabee@aichi-med-u.ac.jp.

[2] The abbreviations used are: ECM, extracellular matrix; HA, hyaluronan; LP, link protein; CS, chondroitin sulfate; HABP, hyaluronan-binding protein; ELISA, enzyme-linked immunosorbent assay; cmd, cartilage matrix deficiency; TBS, Tris-buffered saline.

EXPERIMENTAL PROCEDURES

Immunostaining and Detection of HA by HABP in Tissues—Aggrecan-null cartilage matrix deficiency (cmd) lines (22) were maintained in our animal facility. Mouse tissues were fixed in 10% buffered formalin, embedded in paraffin, and sliced into 4-μm sections. When necessary, hard tissues were decalcified with 0.5 M EDTA for 14 days. For immunostaining, tissue sections were pretreated with 1 unit/ml of protease-free chondroitinase ABC (Seikagaku Corp.) at 37 °C for 30 min. For aggrecan and versican, rabbit polyclonal anti-mouse aggrecan (a gift from Dr. T. Yada, ×500) and anti-mouse versican (anti-CS-α and anti-CS-β, gifts from Dr. T. Shinomura, ×500) were used, respectively. To recognize all three variant forms (V0, V1, and V2) of versican except for V3, which was not expressed as a protein, we used a mixture of anti-CS-α and anti-CS-β antibodies. Biotinylated HABP, ×100; Seikagaku) was used for HA detection. LP immunostaining was performed with mouse monoclonal anti-LP, which reacts with mouse LP (8A4, ×100; Developmental Studies Hybridoma Bank) using HistoMouse™ SP kit (Zymed Laboratory Inc.).

Identification of Proteoglycan Aggregates—Native versican was prepared from mouse brain as described previously (23). In a pilot test of density gradient ultracentrifugation, native versican, biotinylated LP, and HA were best separated at a density of 1.42 mg/ml of CsCl, when versican was fractionated into A1-A3. 220 mg (wet weight) of cmd/cmd cartilage was homogenized in 5 volumes of extraction buffer containing 0.5 M guanidine hydrochloride (GdnHCl), 50 mM Tris-HCl, pH 8.0, 10 mM EDTA, 1 mM phenylmethanesulfonyl fluoride, 10 mM *N*-ethylmaleimide, and 0.36 mM pepstatin A. The homogenate was stirred overnight at 4 °C and clarified by centrifugation in capped polycarbonate tubes (15,000 × *g* 10 min, 4 °C). Solid CsCl was added to give an initial density of 1.42 g/ml, followed by further centrifugation (15,000 × *g*, 10 min, at 4 °C). After the centrifugation, a floating pellicle was removed, and the clarified solutions were centrifuged under an associative condition (0.4 M GdnHCl) in polyallomer tubes at 110,000 × *g*, 10 °C, for 96 h in a swing rotor. The solution in the tube was fractionated into six tubes, A1-A6, from the bottom. To identify these molecules individually, the tissue was extracted using 4 M GdnHCl, Tris-HCl, pH 8.0, 10 mM EDTA, 1 mM phenylmethylsulfonyl fluoride, 10 mM *N*-ethylmaleimide, and 0.36 mM pepstatin A, and the extract was applied to dissociative ultracentrifugation. These molecules were monitored by dot blot and immunoblot analyses. The density of bands and blots was quantified using NIH Image version 1.63. To detect the versican aggregate in articular cartilage, 2-week-old mouse femoral articular cartilage up to 1 mM in depth was carefully dissected and extracted as above, followed by ultracentrifugation at a density of 1.61 g/ml (first centrifugation). The solution was fractionated into 13 tubes, and fractions A9–11 containing versican were collected. The collected sample was ultracentrifuged at 1.61 g/ml again (second centrifugation), and fractions A9–11 were collected and ultracentrifuged again (third centrifugation) at 1.6 g/ml. Then fractions A9–11 containing versican were ultracentrifuged at 1.51 g/ml (fourth centrifugation). Versican, aggrecan, and LP were monitored as above. For quantification of versican and aggrecan in the articular surface area, the surface area at day 14 was carefully excised and extracted using ten volumes of 4 M GdnHCl, 50 mM Tris-HCl, pH 8.0, 10 mM EDTA, 1 mM phenylmethylsulfonyl fluoride, 10 mM *N*-ethylmaleimide, and 0.36 mM pepstatin A for 24 h. The second extraction was then performed using five volumes of the same buffer, which attained almost full extraction. The extract was applied to ELISA as below.

Transfection and Immunostaining of N1511 Cells—N1511 cells were transfected and immunostained as previously described (24). Biotinylated anti-FLAG M2 (×200) and anti-CS-β (×2,000) were used as primary antibodies, followed by treatment with streptavidin- fluorescein isothiocyanate (×1,000) for FLAG or Alexa fluor Texas red (×2,000) for anti-CS-β. Fluorescence was observed using an Olympus BX50 microscope. For HA detection, biotinylated HABP (×500) and streptavidin-fluorescein isothiocyanate (×1,000) were used in place of primary and secondary antibodies, respectively. N1511 cell culture plates were washed three times with phosphate-buffered saline and treated with 10 mM Tris-HCl, pH 8.0, 0.5% sodium deoxycholate, 1 mM phenylmethylsulfonyl fluoride, 1 μg/ml of pepstatin A, and 1 μg/ml of leupeptin. After cell lysis, the remaining matrix was collected and used for immunoblot and dot blot. At day 13 after induction by 1×10^{-6} M dexamethasone (Calbiochem, La Jolla, CA) and 1×10^{-7} M rat parathyroid hormone (Sigma), whole-mount cultures were rinsed with phosphate-buffered saline, fixed with 10% formalin/phosphate-buffered saline for 10 min at room temperature, and then stained with 0.5% Alcian blue (pH 2.0) overnight. Versican was immunostained as above. The area stained with Alcian blue was measured using NIH Image version 1.63.

Quantitative Reverse Transcription PCR—To analyze aggrecan or versican transcription in cartilage, we obtained cartilage from C57/Bl6 mice at days 0 and 2 and at 8 weeks. Poly(A) RNA (200–600 ng) was prepared from cartilage using the Micro-Fast Track™ kit (Invitrogen) and reverse transcribed to generate cDNA using the Superscript II First-Strand Synthesis™ system (Invitrogen). Real-time quantitative PCR was performed using TaqMan™ 7700 (PE Applied Biosystems). Sequences for a probe and a set of primers for versican were chosen by the Primer Express™ program as follows: probe, 5′-CACTCTAACCCTTGTCGGAATGGT-3′; forward primer, 5′-CCAGTGTGAACTTGATTTTGATGAA-3′; and reverse primer, 5′-AACATAACTTGGGAGACAGAGACATCT-3′. The sequences of the probe and primers for aggrecan were described previously (25). The probe was labeled with fluorescent reporter dyes 6-carboxyfluorescein and 6-carboxy-*N,N,N′,N′*-tetramethylrhodamine at 5′- and 3′-ends, respectively. For the internal control, a set of primers and a probe of rodent glyceraldehyde-3-phosphate dehydrogenase labeled with VIC™ (PE Applied Biosystems) were used according to the manufacturer's protocol.

Enzyme-linked Immunosorbent Assay (ELISA)—ELISA plates (MaxiSorp; Nunc) were coated overnight at 4 °C with 100 μl of aggrecan (10 μg/ml; Seikagaku) or versican (5 μg/ml; Collaborative Biomedical Products) in 50 mM Tris-HCl, pH 7.5, 0.15 M NaCl (Tris-buffered saline, TBS) containing 0.2% bovine serum albumin. An anti-aggrecan antibody (×250) or an anti-versican antibody (×250) in 50 ml of TBS containing 0.2% bovine serum albumin was mixed with the same sample volume at different dilutions in TBS containing 0.2% bovine serum albumin and incubated at 37 °C for 1 h. After washing wells with TBS containing 0.05% Tween 20 (TBS-T) three times, the mixture was applied to wells and incubated for 1 h at 37 °C. After washing wells with TBS-T three times, a peroxidase-conjugated goat anti-rabbit antibody (×10,000; Cappel) was applied and incubated for 30 min at 37 °C. After washing wells five times with TBS-T, detection was performed with tetramethylbenzidine (SureBlue™ TMB Microwell Peroxidase Substrate; KPL).

Analysis of CS Disaccharide Composition—Samples fractionated after density gradient ultracentrifugation were precipitated by the addition of 3 volumes of 95% ethanol containing 1.3% potassium acetate. The precipitate was dissolved in distilled water and then treated in 0.2 M NaOH for 24 h at room temperature, neutralized by the addition of 4 M acetate, and then digested with actinase E (Kaken Pharmaceutical) in 50 mM Tris-HCl, pH 8.0, for 5 h at 50 °C. The sample was applied to a DEAE-Sephacel (Amersham Biosciences) column equilibrated with 50 mM Tris-HCl, pH 7.5. After washing with 10 column volumes of 50 mM

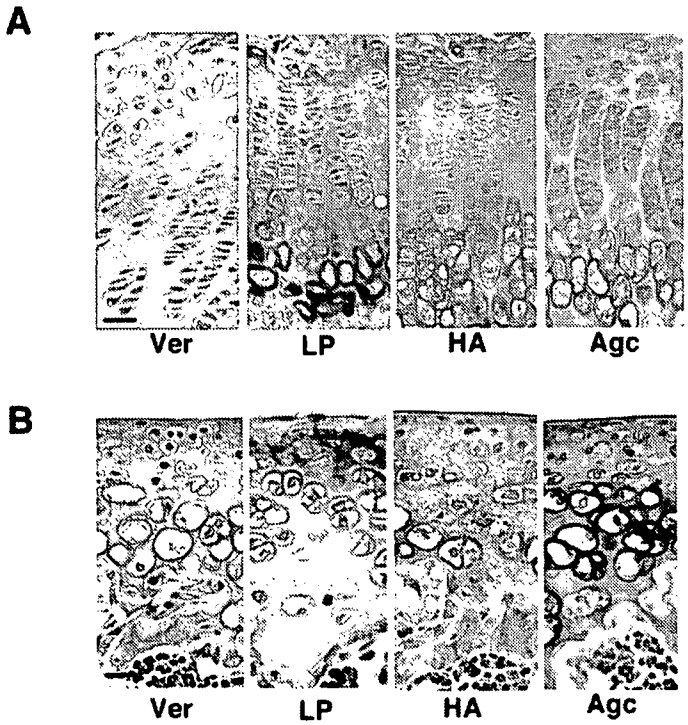

FIGURE 1. **Localization of versican, LP, and HA.** *A*, 2-week-old mouse growth plate (*Bar*, 50 μM). *B*, articular cartilage (*Bar*, 50 μM). Versican, LP, and HA are co-localized in the interterritorial zone of the growth plate and the joint surface.

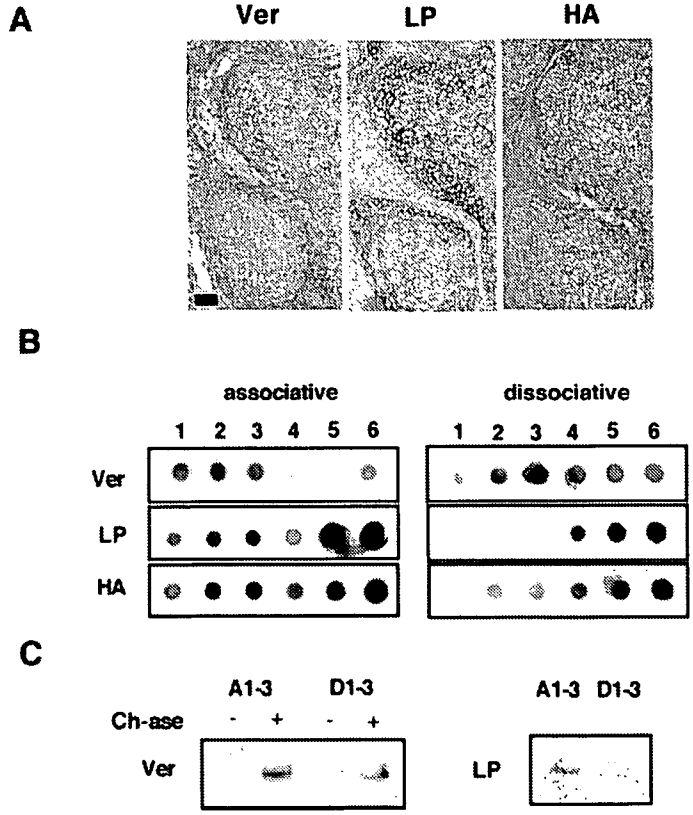

FIGURE 2. **Presence of the versican aggregate in cmd/cmd cartilage.** *A*, co-localization of versican (*Ver*), LP, and HA in newborn cmd/cmd cartilage (*Bar*, 100 μm). *B*, detection of versican (*Ver*), LP, and HA in fractions of density gradient ultracentrifugation under associative (*left*) and dissociative (*right*) conditions. *C*, immunoblot of A1–3 and D1–3 fractions for versican (*Ver*) and LP. Nontreated (−) and chondroitinase ABC-treated (+) samples were applied.

Tris-HCl, pH 7.5, 0.2 M NaCl, GAG-rich fractions were eluted with 50 mM Tris-HCl, pH 7.5, 2 M NaCl. The eluate was ethanol precipitated as above and dissolved in 200 μl of distilled water. The samples were treated with 30 milliunits of chondroitinase ABC in 25 μl of 50 mM Tris-HCl, pH 7.5, 0.04% bovine serum albumin for 4 h at 37 °C and filtered with Ultrafree-MC (5,000 molecular weight limit; Millipore). Unsaturated disaccharides in the filtrates were analyzed by reverse phase ion-pair chromatography using Senshu Pak column Docosil with a fluorescence detector according to the method of Toyoda (26) with slight modification of elution conditions. Separately, we treated the above eluate with hyaluronidase from Streptomyces hyalurolyticus (Seikagaku), similarly filtered and analyzed, and confirmed that hyaluronan disaccharide was negligible in the samples.

RESULTS

Distribution of Versican, HA, and LP in Cartilage—Initially, we investigated the presence and localization of versican, aggrecan, LP, and HA in the growth plate and articular cartilage of 2-week-old mice by immunostaining and with biotinylated hyaluronan-binding protein (biotinylated HABP). In the growth plate, versican was faintly stained in the interterritorial zone. LP was strongly stained in the pericellular zone of hypertrophic chondrocytes and moderately in the interterritorial zone. HA was diffusely localized with higher deposition in the pericellular zone. In contrast, aggrecan was stained mainly in the territorial zone of chondrocyte columns and the pericellular zone of hypertrophic chondrocytes (Fig. 1*A*). In the articular surface, versican, LP, HA, and aggrecan were observed in the interterritorial zone. Aggrecan was also localized in the pericellular zone of hypertrophic cells (Fig. 1*B*). Although the detailed localization of these molecules was different, the colocalization of versican, LP, and HA in the interterritorial zone of the articular surface suggests the presence of their aggregates.

Versican Forms Proteoglycan Aggregates in Vivo—We then examined whether versican is present as a proteoglycan aggregate with HA and LP in cartilage. Because normal cartilage contains a large amount of aggrecan, which may inhibit the identification of versican aggregates, we first used cartilage from cmd/cmd mice (22), a natural knock-out of the aggrecan gene. When the localization of the three molecules in cmd/cmd cartilage was examined, both versican and LP were observed mainly on the cartilage margin, whereas HA was diffuse (Fig. 2*A*), indicating the colocalization of the three molecules at least on the margin of cmd/cmd cartilage. To identify the proteoglycan aggregate, a sample was extracted from cmd/cmd cartilage by 0.5 M GdnHCl and applied to cesium chloride density gradient ultracentrifugation under an associative condition (0.4 M GdnHCl) (27). A major proportion of versican was observed in the A1–3 fractions, and a small proportion, presumably of processed fragments, was found in A6. The major proportion of both LP and HA was seen in A5–6, but some was observed in the A1–3 fractions (Fig. 2*B*, *left*). When the sample extracted by 4 M GdnHCl was ultracentrifuged under dissociative conditions (4 M GdnHCl), a major proportion of versican was observed in the D3 fraction. In contrast, the major proportions of both LP and HA were found in the D5–6 fractions (Fig. 2*B*, *right*). We confirmed the presence of versican and LP by immunoblot analyses. When the A1–3 and D1–3 fractions were treated with chondroitinase ABC and applied to immunoblot, the versican core protein was observed (Fig. 2*C*). LP was observed in the A1–3 fractions but not in D1–3. These data clearly indicate that cmd/cmd cartilage contains the proteoglycan aggregate of versican, LP, and HA.

As the presence of versican aggregates in cmd/cmd may not necessarily indicate their presence in normal cartilage, we attempted to detect versican aggregates in normal cartilage. The surface area of articular cartilage at the age of 2 weeks was extracted under associative condi-

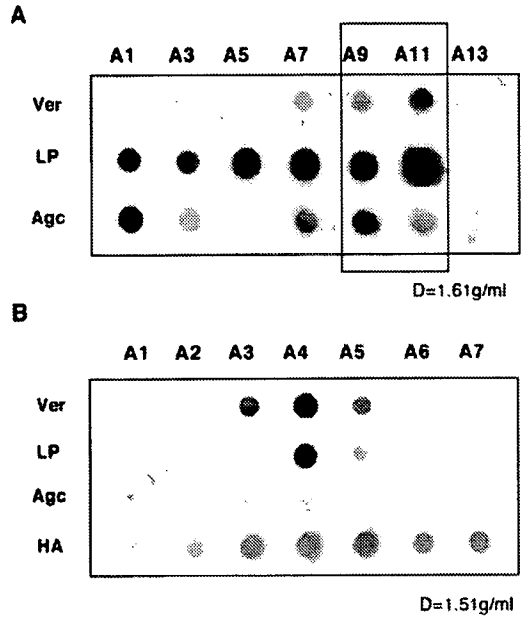

FIGURE 3. **Versican aggregate in normal articular cartilage.** Dot blots of versican (*Ver*), link protein (*LP*), aggrecan, and hyaluronan (*HA*) are shown. *A*, patterns of initial density gradient ultracentrifugation (*d*, 1.61 g/ml) under associative conditions. *B*, patterns of density gradient ultracentrifugation (*d*, 1.51 g/ml) of fractions A9-A10 of the initial ultracentrifugation under associative conditions.

tions and processed by cesium chloride density gradient ultracentrifugation at 1.61 g/ml. Although a large amount of aggrecan was present in A1–3 and A7–11, versican was mainly found in A9–11 (Fig. 3*A*). Repeated ultracentrifugation and collection of versican fractions as described under "Experimental Procedures" successfully removed aggrecan. Subsequent ultracentrifugation at 1.51 g/ml revealed the co-fractionation of both versican and LP mainly in A4 (Fig. 3*B*), indicating the presence of versican aggregates in normal articular cartilage.

Versican and Aggrecan Exhibit Different Sulfation Levels of CS Chains—As cartilage contains two types of proteoglycan aggregates, they may function by harboring different structures of CS chains. We performed disaccharide analysis of CS chains in aggrecan and versican. As both aggrecan-rich (A1–2 in Fig. 3*A*) and versican-rich (A4 in Fig. 3*B*) fractions obtained by repeated density gradient ultracentrifugation were confirmed as being >95% pure, respectively (data not shown), we used these fractions for disaccharide analysis. The GAG sample of the aggrecan-rich fraction treated with chondroitinase ABC contained ~25% ΔdiS-0S and 70% ΔdiS-4S. In contrast, that of the similarly treated versican-rich fraction contained ~71% ΔdiS-0S and 28% ΔdiS-4S. All other disaccharide structures such as ΔdiS-6S, ΔdiS_D, ΔdiS_E, and ΔdiTriS were negligible in both samples (Table 1). These results indicate that both are only sulfated at the 4-position of GalNAc and that sulfation levels of CS chains are higher in aggrecan than versican.

Expression Levels of Versican and Aggrecan in Cartilage—Next, we examined the transcription and protein levels of versican and aggrecan in differently aged mice. Real-time reverse transcription PCR indicated that the levels of versican transcription at 2 and 8 weeks after birth were ~80 and 10%, respectively, that of newborn cartilage, whereas aggrecan transcription gradually increased and at 8 weeks reached 4 times that of the newborn cartilage (Fig. 4*A*). The amount of these proteoglycans was measured in cartilage at different ages by inhibition ELISA. Versican decreased at 2 weeks to ~60% that of newborn cartilage and remained at 8 weeks, whereas the amount of aggrecan/wet weight gradually increased during growth (Fig. 4*B*). These results suggest that versican

TABLE 1
CS disaccharide composition of versican and aggrecan
ND, not determined.

	Versican	Aggrecan
	%	
ΔdiOS	71	25
Δdi4S	28	70
Δdi6S	ND	1
ΔdiS_E	ND	0.4
ΔdiS_D	ND	ND
ΔdiTriS	ND	0.2

remains in the growing cartilage for at least 2–8 weeks after birth, although its transcription dramatically declines.

The samples for quantification above included a mixture of articular and growth plate cartilage. In addition, the amount of these proteoglycans may be different between the surface and deep layers of articular cartilage. Thus we measured their amount in the surface layers (up to 1 mm in depth). Repeated extraction in 4 M GdnHCl confirmed almost full extraction. By inhibition ELISA, the surface area contained 41 and 88 μg/mg (wet weight) of versican and aggrecan, respectively. Interestingly, the extraction efficiency using 0.5 M GdnHCl was 23 and 61%, respectively, suggesting that versican with less CS chains is more tightly incorporated in the cartilage matrix of the articular surface layer.

Deposition of Versican in the ECM Depends on the Expression of LP—Versican is transiently expressed at a high level in the mesenchymal condensation area. After the transcription level rapidly decreases, versican remains in the interterritorial zone of developing cartilage as proteoglycan aggregates. The sustained deposition of versican in the ECM may be dependent on the presence of LP. We tested this hypothesis by overexpressing LP in N1511 chondrogenic cells. Chondrocytic differentiation is induced in these cells by combined treatment with dexamethasone and parathyroid hormone at the confluence (24). After the induction, these cells express versican, peaking at 48 h, and decreasing to 40 and 30% at days 4 and 13, respectively. The expression of aggrecan and LP appears at day 4 with a peak at day 13 (9). Forty-eight hours after the induction, versican and HA deposition in the ECM was observed (Fig. 5*A*) when endogenous LP and aggrecan were not detected (data not shown). Then we transfected subconfluent N1511 cells with an expression vector of human recombinant FLAG-LP. After 24 h, the cells reached confluence and were treated with parathyroid hormone and dexamethasone to induce differentiation. FLAG-LP was overexpressed and incorporated in the matrix and enhanced versican deposition (Fig. 5*A*). When samples of the extracellular matrix were extracted after cell lysis, treated with chondroitinase ABC, and immunoblotted, a significantly increased amount of versican core protein was observed in the matrix where FLAG-LP was overexpressed (Fig. 5*B*). In contrast to versican, HA deposition was not increased when LP was overexpressed (Fig. 5*A*). These results indicate that LP increases versican deposition by forming the proteoglycan aggregate.

Versican Aggregates Inhibit Aggrecan Deposition—Both aggrecan and versican can form aggregates with LP and HA. We examined whether these proteoglycans form a composite aggregate or form their own aggregates in a mutually exclusive manner. We overexpressed FLAG-LP and induced differentiation in N1511 cells. At day 13, a large amount of versican remained in the ECM of LP-expressing cells. The mock-transfected cells showed a round, chondrocyte-like shape in Alcian blue-stained cartilaginous nodules, indicating chondrocyte differentiation with aggrecan deposition. In contrast, LP-expressing cell cultures showed much less Alcian blue-stained nodules (Fig. 6*A*). When the levels of Alcian blue staining were measured, aggrecan deposition was decreased to ~25% in LP-expressing cells (Fig. 6*B*). By immunoblot, the

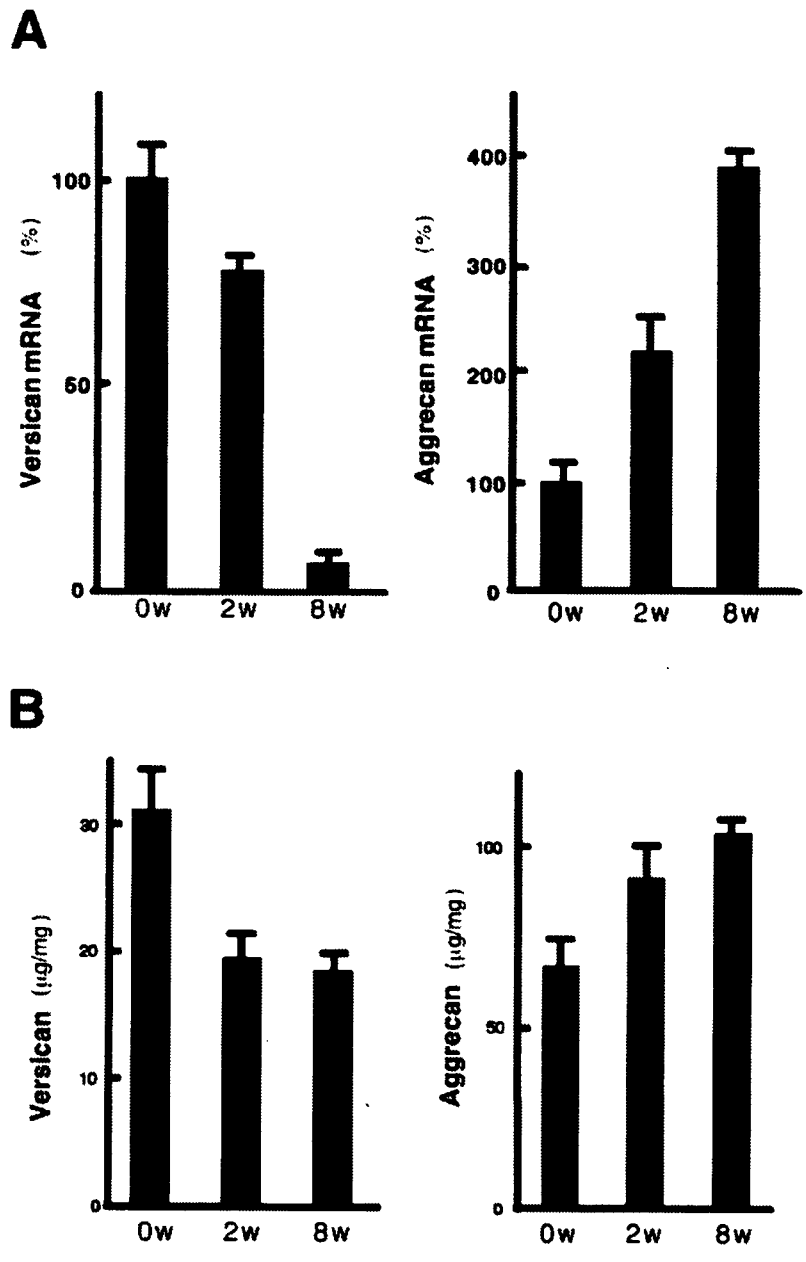

FIGURE 4. **Expression levels of versican and aggrecan in cartilage during growth.** *A*, transcription levels of versican (*left*) and aggrecan (*right*) standardized by those of glyceraldehyde-3-phosphate dehydrogenase are indicated as -folds of day 0 (newborn). *B*, the amounts of versican (*left*) and aggrecan (*right*) per wet weight of cartilage measured by inhibition ELISA are indicated. *2w* and *8w* represent 2 and 8 weeks after birth, respectively.

levels of aggrecan in the conditioned medium of LP-expressing cells were significantly decreased (Fig. 6*C*). These results indicate that sustained deposition of versican aggregates inhibits subsequent aggrecan deposition.

DISCUSSION

In this study, we have shown the presence of versican in cartilage. By immunostaining, versican is localized in the interterritorial zone of the articular surface, whereas aggrecan is mainly in the territorial zone of hypertrophic cells. Biochemical analysis of normal articular and cmd/cmd cartilage revealed that versican is present as a proteoglycan aggregate with both LP and HA. Disaccharide analysis has demonstrated that versican CS is less sulfated than aggrecan CS. *In vitro* studies using chondrocytic N1511 cells demonstrated that LP overexpression at an early stage of differentiation enhanced versican deposition and inhibited subsequent aggrecan deposition. Taken together, these results suggest that cartilage contains both aggrecan aggregates and versican aggregates, which may play their own roles in articular cartilage.

Versican is transiently expressed in the mesenchymal condensation area and is still observed at the epiphyseal end at E15 (8). Although previous immunohistochemical studies failed to detect versican in human adult cartilage (3), biochemical studies demonstrated the presence of versican in human articular cartilage from the fetal stage to mature adult (13). An age-associated decrease in versican transcription of the human articular cartilage has also been reported (11). We have shown that versican is present on the articular surface of mice at 2 weeks after birth. Its transcription in cartilage rapidly decreases from 2- to 8-week-old mice as assessed by real-time quantitative PCR, which may partly be due to a decreased ratio of articular chondrocytes in the total cell population in cartilage. In contrast, deposition remained at 8 weeks. These observations, together with previous reports, suggest that cells on the margin of developing cartilage continuously synthesize versican and may eventually reside as articular chondrocytes and that versican secreted at early stages of life remains in the interterritorial zone of articular cartilage.

We have shown for the first time that versican is present in the form of aggregates with HA and LP in normal articular and cmd/cmd carti-

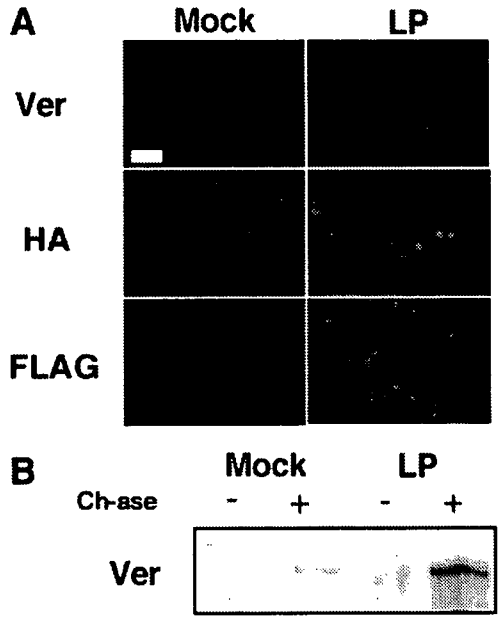

FIGURE 5. **Increase of matrix formation by LP overexpression.** *A*, deposition of versican, HA, and overexpressed LP. FLAG-tagged LP was overexpressed in N1511 cells by transfection at subconfluence (*Bar*, 100 μm), and deposition of ECM molecules was observed at 48 h after the induction of differentiation. *B*, immunoblot of versican at 48 after the induction. After cell lysis, the extracellular matrix was collected and extracted. Samples with or without chondroitinase ABC digestion were immunoblotted for versican.

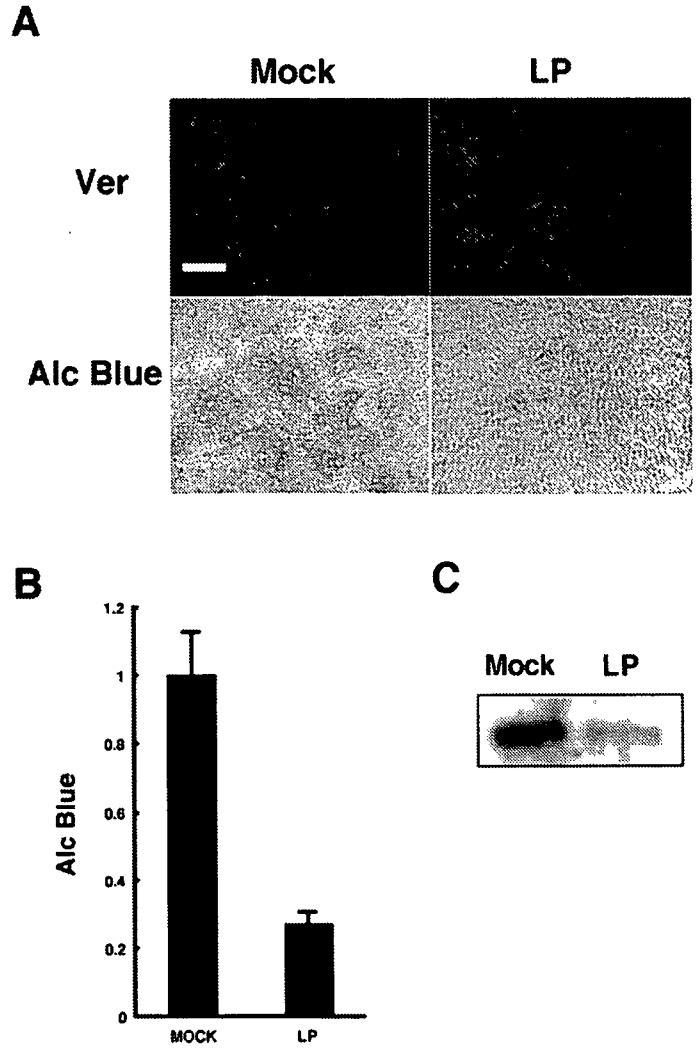

FIGURE 6. **Inhibition of differentiation by increased matrix deposition of versican.** *A*, sustained deposition of versican by overexpression of FLAG-LP (day 13, *upper panels*) and Alcian blue staining patterns (day 13, *lower panels*). *B*, levels of Alcian blue staining, measured by NIH Image. *C*, immunoblot analysis of aggrecan in the conditioned media of mock- and FLAG-LP-transfected cell cultures.

lage, using associative and dissociative CsCl ultracentrifugation methods (28). Extraction under associative conditions followed by ultracentrifugation excludes the possibility of reconstitution of the aggregate during these biochemical procedures. Versican was separated at a density slightly lower than the condition for aggrecan, indicating that this method is useful for the purification of versican in various tissues. Repeated CsCl density gradient ultracentrifugation successfully removed most aggrecan aggregates, and versican was co-fractionated with both HA and LP, suggesting that these proteoglycans are unlikely to form a composite aggregate.

The versican G1 domain interacts with both LP and HA at the B-B′ segment (21) in contrast to aggrecan G1, which binds HA at B-B′ and binds LP at the A subdomain. This different manner of interaction may give rise to the possibility that versican aggregates are replaced with aggrecan aggregates, by exchanging HA and LP. However, our result showing that the sustained deposition of versican aggregates inhibited subsequent aggrecan deposition in differentiating N1511 cells does not support this hypothesis. The versican aggregate is as stable as the aggrecan aggregate, and the interaction of versican with either LP or HA is as strong as that of aggrecan with these molecules (21). Thus, the versican aggregate, once formed, may remain and inhibit further deposition of aggrecan aggregates.

Both aggrecan and versican contain globular domains at both N and C termini. Interaction of these globular domains with other molecules may be necessary to form the framework of the matrix structure, and the amount and structure of CS chains may determine the nature of the matrix. Whereas aggrecan contains >100 CS chains, versican contains up to ~20. In addition, CS chains of versican are less sulfated than those of aggrecan, as shown in this study. Indeed, extraction efficiency of versican by 0.5 M GdnHCl was lower than that of aggrecan. These differences may endow versican with both biochemically and physically specific roles. Versican binds to a greater variety of molecules, including fibronectin (29) and midkine (30), than aggrecan. Recently, transforming growth factor β (TGF-β)/Smad-3 signals have been suggested as essential for repressing articular chondrocyte differentiation. Without this, chondrocytes break the quiescent state and undergo abnormal terminal differentiation (31). As versican is known to bind fibrillin-1 (32), which interacts with latent TGF-β-binding protein-1 (LTBP-1) (33), it may regulate TGF-β-mediated signal transduction through the interaction of fibrillin-1 and LTBP-1. Articular cartilage requires a physical property that resists shear force in the surface area and compression in the deeper zone. Together with compact collagen fibers, versican aggregates, with CS chains of decreased number and sulfation levels compared with aggrecan, may provide an appropriate ECM structure of the articular surface.

The patterns and levels of CS sulfation depend on the activity of chondroitin sulfotransferases in individual cells. Versican from mouse embryos at E13.5 contains 6-sulfated and 4-sulfated disaccharides, comparable with ~90% nonsulfated disaccharides (30). Embryonic chondrocytes may have much less C6-sulfotransferase activity than embryonic fibroblasts. In the same context, versican-expressing articular chondrocytes may have less C4-sulfotransferase activity than aggrecan-expressing chondrocytes.

Versican aggregates in the articular cartilage may provide another important role in destructive joint diseases such as osteoarthritis (34). Because versican is degraded by aggrecanase-1 (a disintegrin and met-

alloproteinase with thrombospondin motif-4, ADAMTS-4) (35), a versican fragment cleaved by the enzyme may serve as a marker for the early stage of arthritis. Further studies are required to understand the *in vivo* roles of versican in cartilage development and homeostasis and in joint destructive diseases.

Acknowledgments—We thank Dr. T. Yada for anti-aggrecan antibody and Dr. Z. D. Zhang, H. Fuwa, and S. Hara for technical assistance.

REFERENCES

1. Zimmermann, D. R., and Ruoslahti, E. (1989) *EMBO J.* **8,** 2975–2981
2. Shinomura, T., Nishida, Y., Ito, K., and Kimata, K. (1993) *J. Biol. Chem.* **268,** 14461–14469
3. Bode-Lesniewska, B., Dours-Zimmermann, M. T., Odermatt, B. F., Briner, J., Heitz, P. U., and Zimmermann, D. R. (1996) *J. Histochem. Cytochem.* **44,** 303–312
4. Yamagata, M., Saga, S., Kato, M., Bernfield, M., and Kimata, K. (1993) *J. Cell Sci.* **106,** Pt. 1, 55–65
5. Landolt, R. M., Vaughan, L., Winterhalter, K. H., and Zimmermann, D. R. (1995) *Development* **121,** 2303–2312
6. Kishimoto, J., Ehama, R., Wu, L., Jiang, S., Jiang, N., and Burgeson, R. E. (1999) *Proc. Natl. Acad. Sci. U. S. A.* **96,** 7336–7341
7. Kimata, K., Oike, Y., Tani, K., Shinomura, T., Yamagata, M., Uritani, M., and Suzuki, S. (1986) *J. Biol. Chem.* **261,** 13517–13525
8. Shibata, S., Fukada, K., Imai, H., Abe, T., and Yamashita, Y. (2003) *J. Anat.* **203,** 425–432
9. Kamiya, N., Watanabe, H., Habuchi, H., Takagi, H., Shinomura, T., Shimizu, K., and Kimata, K. (2006) *J. Biol. Chem.* **281,** 2390–2400
10. Wight, T. N., Heinegård, D. K., and Hascall, V. C. (1991) in *Cell Biology of Extracelulat Matrix* (Hay, E. D., ed) 2nd Ed., pp. 45–78, Plenum Press, New York
11. Grover, J., and Roughley, P. J. (1993) *Biochem. J.* **291,** Pt. 2, 361–367
12. Kolettas, E., Buluwela, L., Bayliss, M. T., and Muir, H. I. (1995) *J. Cell Sci.* **108,** Pt. 5, 1991–1999
13. Sztrolovics, R., Grover, J., Cs-Szabo, G., Shi, S. L., Zhang, Y., Mort, J. S., and Roughley, P. J. (2002) *J. Orthop. Res.* **20,** 257–266
14. Watanabe, H., Cheung, S. C., Itano, N., Kimata, K., and Yamada, Y. (1997) *J. Biol. Chem.* **272,** 28057–28065
15. Aspberg, A., Adam, S., Kostka, G., Timpl, R., and Heinegard, D. (1999) *J. Biol. Chem.* **274,** 20444–20449
16. Olin, A. I., Morgelin, M., Sasaki, T., Timpl, R., Heinegard, D., and Aspberg, A. (2001) *J. Biol. Chem.* **276,** 1253–1261
17. Aspberg, A., Miura, R., Bourdoulous, S., Shimonaka, M., Heinegard, D., Schachner, M., Ruoslahti, E., and Yamaguchi, Y. (1997) *Proc. Natl. Acad. Sci. U. S. A.* **94,** 10116–10121
18. Day, J. M., Olin, A. I., Murdoch, A. D., Canfield, A., Sasaki, T., Timpl, R., Hardingham, T. E., and Aspberg, A. (2004) *J. Biol. Chem.* **279,** 12511–12518
19. Ujita, M., Shinomura, T., Ito, K., Kitagawa, Y., and Kimata, K. (1994) *J. Biol. Chem.* **269,** 27603–27609
20. Evanko, S. P., Johnson, P. Y., Braun, K. R., Underhill, C. B., Dudhia, J., and Wight, T. N. (2001) *Arch. Biochem. Biophys.* **394,** 29–38
21. Matsumoto, K., Shionyu, M., Go, M., Shimizu, K., Shinomura, T., Kimata, K., and Watanabe, H. (2003) *J. Biol. Chem.* **278,** 41205–41212
22. Watanabe, H., Kimata, K., Line, S., Strong, D., Gao, L. Y., Kozak, C. A., and Yamada, Y. (1994) *Nat. Genet.* **7,** 154–157
23. Schmalfeldt, M., Dours-Zimmermann, M. T., Winterhalter, K. H., and Zimmermann, D. R. (1998) *J. Biol. Chem.* **273,** 15758–15764
24. Kamiya, N., Jikko, A., Kimata, K., Damsky, C., Shimizu, K., and Watanabe, H. (2002) *J. Bone Miner Res.* **17,** 1832–1842
25. Watanabe, H., de Caestecker, M. P., and Yamada, Y. (2001) *J. Biol. Chem.* **276,** 14466–14473
26. Toyoda, H., Kinoshita-Toyoda, A., and Selleck, S. B. (2000) *J. Biol. Chem.* **275,** 2269–2275
27. Faltz, L. L., Reddi, A. H., Hascall, G. K., Martin, D., Pita, J. C., and Hascall, V. C. (1979) *J. Biol. Chem.* **254,** 1375–1380
28. Hascall, V. C., and Kimura, J. H. (1982) *Methods Enzymol.* **82,** Pt. A, 769–800
29. Yamagata, M., Suzuki, S., Akiyama, S. K., Yamada, K. M., and Kimata, K. (1989) *J. Biol. Chem.* **264,** 8012–8018
30. Zou, K., Muramatsu, H., Ikematsu, S., Sakuma, S., Salama, R. H., Shinomura, T., Kimata, K., and Muramatsu, T. (2000) *Eur. J. Biochem.* **267,** 4046–4053
31. Yang, X., Chen, L., Xu, X., Li, C., Huang, C., and Deng, C. X. (2001) *J. Cell Biol.* **153,** 35–46
32. Isogai, Z., Aspberg, A., Keene, D. R., Ono, R. N., Reinhardt, D. P., and Sakai, L. Y. (2002) *J. Biol. Chem.* **277,** 4565–4572
33. Isogai, Z., Ono, R. N., Ushiro, S., Keene, D. R., Chen, Y., Mazzieri, R., Charbonneau, N. L., Reinhardt, D. P., Rifkin, D. B., and Sakai, L. Y. (2003) *J. Biol. Chem.* **278,** 2750–2757
34. Nishida, Y., Shinomura, T., Iwata, H., Miura, T., and Kimata, K. (1994) *Osteoarthritis Cartilage* **2,** 43–49
35. Sandy, J. D., Westling, J., Kenagy, R. D., Iruela-Arispe, M. L., Verscharen, C., Rodriguez-Mazaneque, J. C., Zimmermann, D. R., Lemire, J. M., Fischer, J. W., Wight, T. N., and Clowes, A. W. (2001) *J. Biol. Chem.* **276,** 13372–13378

THE JOURNAL OF BIOLOGICAL CHEMISTRY VOL. 282, NO. 6, pp. 4152–4161, February 9, 2007

Chondroitin Sulfate *N*-Acetylgalactosaminyltransferase-1 Plays a Critical Role in Chondroitin Sulfate Synthesis in Cartilage*[S]

Received for publication, July 19, 2006, and in revised form, October 23, 2006 Published, JBC Papers in Press, December 4, 2006, DOI 10.1074/jbc.M606870200

Kenichiro Sakai[‡§], Koji Kimata[‡], Takashi Sato[¶], Masanori Gotoh[¶], Hisashi Narimatsu[¶], Kenichi Shinomiya[§], and Hideto Watanabe[‡1]

From the [‡]Institute for Molecular Science of Medicine, Aichi Medical University, Nagakute, Aichi 480-1195, Japan, the [§]Department of Orthopedic Surgery, Tokyo Medical and Dental University, Bunkyo-ku, Tokyo 113-8519, Japan, and the [¶]Research Center for Glycoscience, National Institute of Advanced Industrial Science and Technology, Tsukuba, Ibaraki 305-8568, Japan

Cartilage destruction leads to severe joint diseases, such as osteoarthritis and spinal disorders with back pain, and cartilage regeneration is very inefficient. A major component of the cartilage extracellular matrix is the proteoglycan aggrecan that contains approximately 100 chondroitin sulfate (CS) chains, which impart water absorption and resistance to compression. Here, we demonstrate that chondroitin sulfate *N*-acetylgalactosaminyltransferase-1 (CSGalNAcT-1) plays a critical role in CS biosynthesis in cartilage. By *in situ* hybridization and real time reverse transcription-PCR of developing cartilage, CSGalNAcT-1 exhibited the highest level of expression. Its expression in chondrogenic ATDC5 cells correlated well with that of aggrecan core protein. In heterozygote and homozygote aggrecan-null cartilage where aggrecan transcription is decreased, CSGalNAcT-1 transcription diminished accordingly. Overexpression of the enzyme in chondrocytic cells further enhanced CS biosynthesis but not that of the aggrecan core protein, indicating that the enzyme activity is not saturated in the cells and that aggrecan synthesized in the overexpressing cells is heavier than the native molecule. Analysis of the CS chains synthesized in the overexpressing cells by gel chromatography and that of disaccharide composition revealed that the CS chains had similar length and sulfation patterns. Furthermore, adenoviral gene delivery of the enzyme into intervertebral discs displayed a substantial increase in the level of CS biosynthesis. These observations indicate that CSGalNAcT-1 overexpression increases the number of CS chains attached to aggrecan core protein. Our studies may lead to a new therapeutic intervention, ameliorating the outcome of cartilage degenerative diseases.

Cartilage is localized on joint surfaces and in the spine, where it forms the intervertebral discs and helps physical movement. The extracellular matrix of cartilage contains two major structural components: the fiber structure made of collagens and the proteoglycan aggregate. Whereas collagen fibers of types II, IX, and XI provide cartilage with tensile strength, the proteoglycan aggregate, composed of a large proteoglycan aggrecan, hyaluronan, and link protein, provides it with resistance to compression (1). Aggrecan consists of a core protein and approximately 100 chains of chondroitin sulfate (CS)[2] attached to the core protein (2, 3). Aggrecan is incorporated into the cartilage matrix by binding hyaluronan, and the CS chains impart water absorption. The CS content of aggrecan gradually diminishes with age, resulting in decreased water retention and aggravation of cartilage degeneration (4–6). This leads to severe joint diseases, such as osteoarthritis (7, 8) and spinal disorders with back pain (9, 10). Due to the lack of blood vessels and the presence of specific structural macromolecules, such as aggrecan, cartilage is one of the most difficult tissues to regenerate.

CS comprises repeating disaccharide units of GalNAc and glucuronic acid (GlcUA) residues with sulfate residues at various positions. CS biosynthesis (11) (Fig. 1*A*) is initiated by the transfer of a GalNAc residue to the linkage region of a GlcUA-β1,3-Gal-β1,3-Gal-β1,4-Xyl tetrasaccharide primer that is attached to a serine residue of the core protein. Then chain elongation occurs by the alternate addition of GalNAc and GlcUA residues. Enzyme activities that catalyze the initiation and elongation processes are termed glycosyltransferase-I and II activities, respectively (12). To date, six glycosyltransferases involved in CS synthesis have been identified (Fig. 1*B*): chondroitin sulfate synthase-1 (CSS-1)/chondroitin synthase (13), chondroitin sulfate synthase-2 (CSS-2)/chondroitin-polymerizing factor (14, 15), chondroitin sulfate synthase-3 (CSS-3) (16), chondroitin sulfate glucuronyltransferase (CSGlcAT) (17), and chondroitin sulfate *N*-acetylgalactosaminyltransferase-1 (18, 19) and -2 (20, 21) (CSGalNAcT-1 and -2, respectively). All of these enzymes have an N-terminal transmembrane domain and are localized to the Golgi apparatus, where CS biosyn-

* This work was supported by the New Energy and Industrial Technology Development Organization and by grants-in-aid for scientific research (C) (KAKENHI) (to H. W). The costs of publication of this article were defrayed in part by the payment of page charges. This article must therefore be hereby marked "*advertisement*" in accordance with 18 U.S.C. Section 1734 solely to indicate this fact.

[S] The on-line version of this article (available at http://www.jbc.org) contains supplemental Tables 1–3.

[1] To whom correspondence should be addressed: Institute for Molecular Science of Medicine, Aichi Medical University, Nagakute, Aichi 480-1195, Japan. Tel.: 81-561-62-3311 (ext. 2086); Fax: 81-561-63-3532; E-mail: wannabee@aichi-med-u.ac.jp.

[2] The abbreviations used are: CS, chondroitin sulfate; GlcUA, glucuronic acid; CSS-1, -2, and -3, chondroitin sulfate synthase-1, -2, and -3, respectively; CSGlcAT, chondroitin sulfate glucuronyltransferase; CSGalNAcT-1 and -2, chondroitin sulfate *N*-acetylgalactosaminyltransferase-1 and -2, respectively; GalNAcT, *N*-acetylgalactosaminyltransferase; GlcAT, glucuronyltransferase; cmd, cartilage matrix deficiency; RT, reverse transcription; HexA, hexuronic acid; E*n*, embryonic day *n*.

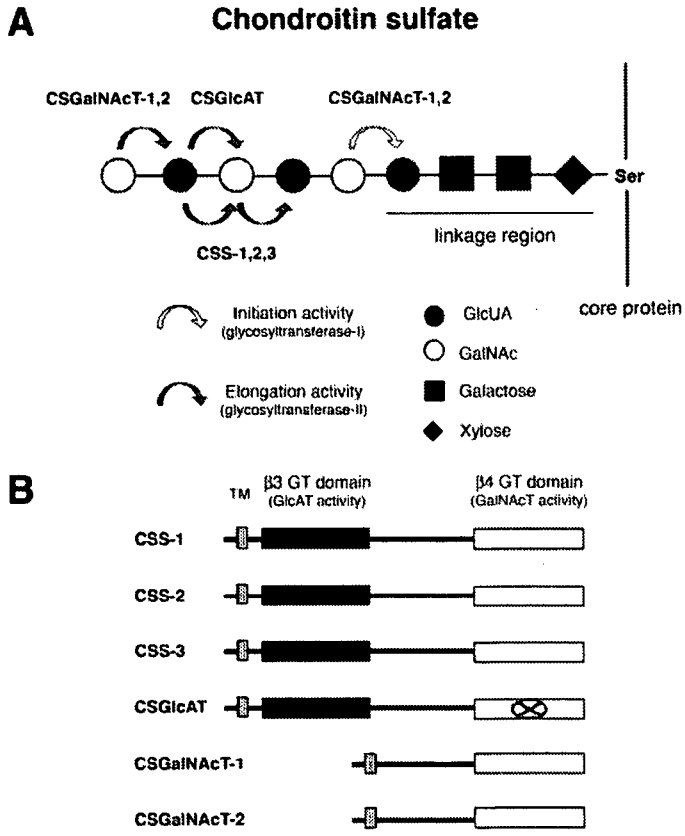

FIGURE 1. **CS biosynthesis and its related glycosyltransferases.** *A*, a schematic diagram of the catalytic activities of the glycosyltransferases involved in chondroitin sulfate synthesis. CS biosynthesis is initiated by the transfer of a GalNAc unit to the linkage region of a GlcUA-Gal-Gal-Xyl tetrasaccharide primer that is attached to a serine residue of the core protein. This is followed by chain elongation that occurs by the alternate addition of GalNAc and GlcUA residues. Six glycosyltransferases involved in CS synthesis have been identified. CSS-1, -2, and -3 exhibit both GalNAcT and GlcAT activities in chain elongation (glycosyltransferase-II activity). CSGlcAT exhibits only GlcAT-II activity. CSGalNAcT-1 and -2 exhibit GalNAcT activity in both the initiation and elongation processes (GalNAcT-I and -II activities). *B*, a schematic structural comparison of the six glycosyltransferases. Conserved domains in β1,3-galactosyltransferases or β1,4-galactosyltransferases are indicated as *closed* or *open boxes*. The putative transmembrane (*TM*) domains are indicated as *gray boxes*.

thesis takes place (22). CSS-1, CSS-2, CSS-3, and CSGlcAT form a family of glycosyltransferase enzymes. CSS-1, CSS-2, and CSS-3 contain two glycosyltransferase domains and exhibit both *N*-acetylgalactosaminyltransferase (GalNAcT) and glucuronyltransferase (GlcAT) activities in chain elongation. Thus, they have glycosyltransferase-II (both GalNAcT-II and GlcAT-II) activity. CSGlcAT has an inactive GalNAcT domain and exhibits only GlcAT-II activity. CSGalNAcT-1 and -2 have one glycosyltransferase domain and exhibit GalNAcT activity in both the initiation and elongation processes, indicating that CSGalNAcT-1 and -2 have both GalNAcT-I and -II activities. Thus, CS chain elongation may involve all six enzymes, whereas CS chain initiation probably involves only CSGalNAcT-1 and -2. Although individual enzymes have been biochemically characterized, the *in vivo* mechanism of CS biosynthesis is not fully understood. Since cartilage contains a large amount of CS, chondrocytes must be capable of efficiently synthesizing numerous CS chains. Elucidation of the mechanism of CS biosynthesis in cartilage would provide a basis for the development of a treatment promoting cartilage regeneration.

In this study, we identified CSGalNAcT-1 as the enzyme critical for cartilage CS biosynthesis. Overexpression of the enzyme in chondrocytic cells elevated the level of CS biosynthesis, and *in vivo* adenoviral gene delivery of the enzyme into the intervertebral disc resulted in a higher level of CS incorporation. The aggrecan synthesized in the CSGalNAcT-1-overexpressing cells had a higher number of CS chains. We term this molecule "superaggrecan" and propose a novel enzyme-based approach for the therapeutic intervention of cartilage degenerative diseases.

EXPERIMENTAL PROCEDURES

In Situ Hybridization—cDNA fragments encoding glycosyltransferases and aggrecan core protein were prepared by PCR using cDNA of differentiating ATDC5 cells and appropriate primers (supplemental Table 1). The PCR product was then subcloned into the pBluescript IISK(−) vector (Stratagene). RNA probes were prepared using cDNA prepared as described above and a DIG RNA labeling kit (Roche Applied Science). A humerus was obtained from an E16.5 mouse and fixed with 4% paraformaldehyde for 16 h at 4 °C. The samples were embedded in paraffin and sliced into 4-μm sections. *In situ* hybridization was performed as described previously (23).

Cell Culture—ATDC5 cells, a cell line established from chondrocytic cells of a mouse embryonal carcinoma, undergo all of the steps of chondrogenesis (24). The cells were cultured in a maintenance medium consisting of a 1:1 mixture of Dulbecco's modified Eagle's medium and Ham's F-12 medium containing 5% fetal bovine serum, 10 μg/ml human transferrin, 3×10^{-8} M sodium selenite, penicillin, and streptomycin. To induce chondrocyte differentiation, the cells at confluence were treated with 10 μg/ml of bovine insulin. N1511 cells, a cell line established from chondrocytic cells from the rib cage of a 4-week-old male p53-null mouse, undergo all of the steps of chondrogenesis (25). The cells were cultured in minimum essential medium α supplemented with 10% fetal bovine serum, penicillin, and streptomycin. Differentiation was similarly induced by combined treatment with of 1×10^{-6} M dexamethasone and 1×10^{-7} M rat parathorimone. LTC cells, a rat chondrosarcoma cell line, were cultured in Ham's F-12 medium containing 10% fetal bovine serum, penicillin, and streptomycin. 293A cells, an embryonic human kidney cell line, were cultured in Dulbecco's modified Eagle's medium containing 10% fetal bovine serum, 0.1 mM minimum essential medium nonessential amino acids, 2 mM L-glutamine, penicillin, and streptomycin. Cell culture was performed at 37 °C in a humidified atmosphere of 5% CO_2 in air. The medium was changed every other day.

Real Time RT-PCR—mRNA was isolated from ATDC5, N1511, and transfected LTC cells and cartilage of a cartilage matrix deficiency (cmd) mouse at E18.5 using Micro-Fast-Track™ (Invitrogen) according to the manufacturer's instructions. cDNA was synthesized using SuperScript™ First-Strand (Invitrogen) according to the manufacturer's instructions. The TaqMan probes contained a reporter dye at the 5′ end and a quencher dye at the 3′ end. To calculate the copy number, control vectors were prepared by PCR using appropriate primers and the cDNA obtained from N1511 cells, followed by subcloning of the fragment into pCRII-TOPO (Invitrogen). For CSS-3,

a BAC clone was used as the PCR template. Primers and probes used for real time RT-PCR are listed in supplemental Table 2. Primers for the control vector are listed in supplemental Table 3. Relative quantification of gene expression was performed using the Applied Biosystems ABI Prism 7700 sequence detection system (TaqMan). PCRs for all of the samples were performed in triplicate in 96-well optical plates using 5 ng of cDNA, 25 μl of TaqMan Universal PCR Mastermix (Applied Biosystems), 100 nM probe, 100 nM each primer, and water to a final volume of 50 μl. Thermocycling conditions comprised an initial holding step at 50 °C for 2 min, 95 °C for 10 min, and 50 cycles of 95 °C for 15 s and 60 °C for 60 s. To standardize mRNA levels, the primers for glyceraldehyde-3-phosphate dehydrogenase were used as internal controls.

Construction of Mammalian Expression Vectors of Glycosyltransferases and Establishment of Their Overexpressing Cell Lines—Full-length human cDNA encoding the glycosyltransferases was amplified by PCR using the Marathon Ready™ cDNA obtained from human bone marrow tissue (Clontech) as the template and two primers: 5′-AAGCTTCCCAAGCTTATGATGATGGTTCGCCGGGGGCT-3′ and 5′-TCTAGAGCTCTAGATCATGTTTTTTTGCTACTTGTCTTCTGT-3′ for CSGalNAcT-1; 5′-AAGCTTCCCAAGCTTGCGGGCATGGCCGCGCGCGG-3′ and 5′-TCTAGAGCTCTAGACATTAGGCTGTCCTCACTGA-3′ for CSS-1; 5′-AAGCTTCCCAAGCTTATGCGGGCATCGCTGCTGCTGT-3′ and 5′-TCTAGACGGGATCCTCAGGTGCTGTTGCCCTGCTCC-3′ for CSS-2; 5′-AAGCTTCCCAAGCTTACCACCATGCGACTGAGCTCCCT-3′ and 5′-TCTAGAGCTCTAGACTAAGTGCTATTGGCCTGCTCCT-3′ for CSGlcAT, which are attached with a HindIII or XbaI site (underlined), respectively. The amplified fragment was subcloned into pcDNA/Hygro (Invitrogen) using the HindIII and XbaI sites, as previously described (20). The CSGalNAcT-1/pcDNA3.1(+), CSS-1/pcDNA3.1(+), CSS-2/pcDNA3.1(+), and CSGlcAT/pcDNA3.1(+) vectors were constructed by subcloning the full-length cDNA into pcDNA3.1 (Invitrogen). LTC cells were transfected with these expression vectors (+) or pcDNA3.1(+) (as a mock control) using FuGENE6 (Roche Applied Science) according to the manufacturer's instructions. These cells were cultured in the presence of 750 μg/ml G418 (Nacalai) for 10 days. The expression levels of these enzymes were measured by real time RT-PCR. The stable cells overexpressing individual enzymes at similar levels were used.

Alcian Blue Staining—Cells were plated in 35-mm dishes. When the cells reached 80% confluence in a conditioned medium on day 2, they were washed in phosphate-buffered saline and fixed with 4% paraformaldehyde for 30 min. A humerus was obtained from an E16.5 mouse and fixed with 4% paraformaldehyde for 16 h at 4 °C. The samples were embedded in paraffin and sliced into 4-μm sections. Transduced vertebral sections were obtained as described below. The cells and deparaffinized sections were then stained using 0.1% Alcian blue in 0.1 M HCl at room temperature for 10 min.

Immunostaining—The transfected LTC cells were plated in 4-well culture slides. When the cells reached 30% confluence at day 2, they were washed in phosphate-buffered saline and fixed with 4% paraformaldehyde for 30 min. They were double-immunostained as previously described (25). For chondroitin 4-sulfate detection, mouse monoclonal anti-chondroitin 4-sulfate (LY111, ×200; Seikagaku) and Alexa Fluor™ 488-conjugated anti-mouse IgM (×1000) were used as the primary and secondary antibodies, respectively. For aggrecan core protein detection, rabbit polyclonal anti-aggrecan (×1000) (26) and Alexa Fluor™ 594-conjugated anti-rabbit IgG (×1000) were used as the primary and secondary antibodies, respectively. The specimen was observed using a Zeiss LSM 5 Pascal laser confocal microscope.

Characterization of Aggrecan—The transfected LTC cells were plated in a 100-mm culture dish. The cells and conditioned medium were collected separately at day 2 and extracted with 4 M guanidine hydrochloride, 50 mM Tris-HCl, pH 8.0, 10 mM EDTA, 1 mM phenylmethanesulfonyl fluoride, and 10 mM *N*-ethylmaleimide. The samples were stirred overnight at 4 °C and clarified by centrifugation in capped polycarbonate tubes (15,000 × *g*, 10 min, 4 °C). Portions of the samples were used for immuno-dot blot analysis. CsCl was added to obtain a density of 1.55 g/ml, and this was followed by ultracentrifugation under a dissociative condition in polyallomer tubes at 40,000 × *g* at 10 °C for 70 h. This ultracentrifugation at a slightly higher density enabled separation of the various aggrecan populations. The solution in the tube was fractionated into nine tubes (D1–D9) from the bottom. Aggrecan separation was monitored by immuno-dot blot analysis.

Immuno-dot Blot Analysis—The samples were applied to nylon N^+ membranes by dot blot using the BIO-DOT™ apparatus (Bio-Rad). The membranes were immunodetected as previously described with slight modification (4). They were pretreated with 1 unit/ml protease-free chondroitinase ABC (Seikagaku). For aggrecan core protein detection, rabbit polyclonal anti-aggrecan (×5000) and peroxidase-conjugated goat anti-rabbit IgG (×10,000; Cappel) were used as the primary and secondary antibodies, respectively.

Characterization of CS Chains—The transfected LTC cells were plated in a 100-mm culture dish. After 2 days, they were labeled with [^{35}S]sulfate (100 μCi/ml) for 24 h. The cells and conditioned medium were collected separately at day 3 and extracted with 0.2 M NaOH for 16 h at room temperature. Next, they were neutralized by the addition of 4 M acetate and digested with 1 mg/ml proteinase K in 50 mM Tris-HCl, pH 8.0, for 2 h at 37 °C. The samples were applied to a DEAE-Sephacel (Amersham Biosciences) column that was equilibrated with 50 mM Tris-HCl, pH 7.5. After washing with 10 column volumes of 50 mM Tris-HCl, pH 7.5, 0.2 M NaCl, glycosaminoglycan-rich fractions were eluted with 50 mM Tris-HCl, pH 7.5, 2 M NaCl. The eluates were precipitated by the addition of 3 volumes of 95% ethanol containing 1.3% potassium acetate, and the precipitate was dissolved in 1 ml of distilled water. A portion (100 μl) of the sample was further isolated by treatment with a mixture of 10 microunits/ml heparitinase I (Seikagaku), 5 microunits/ml, heparitinase II (Seikagaku), and 10 microunits/ml heparinase (Seikagaku) in 20 mM acetate buffer, pH 7.0, 2 mM calcium acetate for 2 h at 37 °C. Separation was performed using an Ultrafree-MC filter cup (Millipore) and dissolved in 200 μl of distilled water. To evaluate [^{35}S]sulfate incorporation, a portion (100 μl) of the sample was measured by scintillation counting. To examine the chain lengths, the other portion (100 μl) of the

sample was applied to a Superose 6 column (Amersham Biosciences) equilibrated in 50 mM Tris-HCl, pH 7.5, and 0.2 M NaCl. Elution of the CS chains was monitored by scintillation counting. In separate experiments, heparitinase-resistant glycosaminoglycan fractions were prepared from the conditioned medium of nonlabeled LTC cells as described above. The sample was labeled with ^{3}H-labeled sodium borohydride as described previously (27). After the removal of free ^{3}H-labeled sodium borohydride using a Sephadex G-25 spin column, the labeled sample (~90,000 cpm) was applied to a Superose 6 column under the same conditions as above.

Analysis of CS Disaccharide Composition—Transfected LTC cells were plated in a 100-mm culture dish. The cells and conditioned medium were collected separately at day 2. Glycosaminoglycans were isolated by β-elimination, protease digestion, and DEAE-Sephacel column chromatography, as described above. The eluates were precipitated by the addition of 3 volumes of 95% ethanol containing 1.3% potassium acetate, and the precipitate was dissolved in 100 μl of distilled water. The samples were treated with 30 milliunits of chondroitinase ABC in 25 μl of 50 mM Tris-HCl, pH 7.5, 0.04% bovine serum albumin for 2 h at 37 °C, and filtered using Ultrafree-MC (5,000 molecular weight limit). Unsaturated disaccharides in the filtrates were analyzed by reverse phase ion pair chromatography using the Senshu Pak column Docosil with a fluorescence detector according to Toyoda's method (28) with a slight modification of elution conditions. The modified gradient program was as follows: 0–10 min, 1–4% eluent B; 10–11 min, 4–10% eluent B; 11–20 min, 10–18% eluent B; 20–22 min, 18–70% eluent B; 22–29 min, 70% eluent B.

Construction of the CSGalNAcT-1 Adenovirus Expression Vector, Viral Particle Production, and in Vivo Transduction to Vertebral Disc—cDNA encoding human CSGalNAcT-1 was prepared by PCR using the primers (5′-CACCATGATGATGGTTCGCCG-3′, 5′-TGTTTTTTTGCTACTTGTCTTCTG-3′) and CSGalNAcT-1/pcDNA3.1(+) as the template. This cDNA was then subcloned into pAd/CMV/V5-DEST (Invitrogen) using pENT/D-TOPO (Invitrogen). Adenoviral particles were obtained by transfecting 293A cells with the CSGalNAcT-1 adenoviral expression plasmid, and the titer was checked according to the manufacturer's instructions (ViraPower™ adenoviral expression system; Invitrogen). Adenoviral particles prepared using pAd/CMV/V5-GW/Lac-Z (Invitrogen) were used as the negative control. The particles (1.5×10^7 plaque-forming units) were injected into the caudal intervertebral discs of 4-month-old ICR mice. One week after the injection, the mice were sacrificed, and the caudal vertebrae were immersed in 4% paraformaldehyde at 4 °C overnight and decalcified with K-CX solution (Fujisawa) for 24 h at room temperature. The samples were then embedded in paraffin and sliced into 4-μm sections.

RESULTS

Expression Patterns of Glycosyltransferases Involved in CS Biosynthesis in Cartilage—The growth plate cartilage contains chondrocytes at different stages of differentiation: resting, proliferative, prehypertrophic, and hypertrophic chondrocytes (29). During differentiation, chondrocytes at the prehypertrophic stage show the highest level of aggrecan synthesis (30). Since the CS chains are attached to the core protein of aggrecan in cartilage, the expression of the key enzymes required for CS biosynthesis is probably up-regulated, correlating with the expression of aggrecan core protein during chondrocyte differentiation. Initially, we investigated the expression of glycosyltransferases involved in CS biosynthesis in mouse developing cartilage. By *in situ* hybridization, CSS-1, CSS-2, CSGlcAT, and CSGalNAcT-1 were shown to be expressed in the prehypertrophic zone of the growth plate at E16.5, colocalized with aggrecan core protein. In particular, CSGalNAcT-1 was expressed at the highest level. In contrast, CSS-3 and CSGalNAcT-2 were expressed at very low levels (Fig. 2).

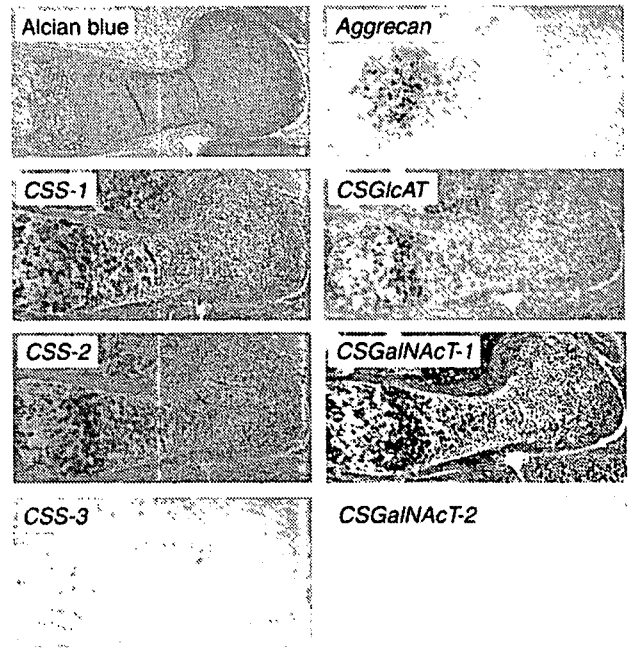

FIGURE 2. ***In situ* hybridization patterns of the glycosyltransferases involved in CS biosynthesis and aggrecan core protein in developing cartilage.** The expression patterns of aggrecan core protein (*Aggrecan*), CSS-1, CSS-2, CSS-3, CSGlcAT, and CSGalNAcT-1 and -2 in a mouse humerus at E16.5 are shown together with the staining pattern with Alcian blue. Note that CSS-1, CSS-2, CSGlcAT, and CSGalNAcT-1 are expressed in the prehypertrophic zone of the growth plate at E16.5 and colocalized with aggrecan core protein. CSGalNAcT-1, in particular, showed the highest level of expression.

Next, we examined the expression patterns of the CS biosynthetic enzymes in ATDC5 cells, which reflect the *in vivo* chondrocyte differentiation process (24, 31). The expression of both CSGlcAT and CSGalNAcT-1 was increased similar to that of aggrecan core protein, whereas response was less pronounced for that of CSS-1, CSS-2, and CSGalNAcT-2. The expression of CSS-3 was not detected (Fig. 3). Another chondrogenic cell line N1511 (25) displayed expression patterns similar to those of CS biosynthetic enzymes during differentiation (data not shown). These *in vitro* cell culture results indicate that the expression of CSGlcAT and CSGalNAcT-1 correlates well with that of aggrecan core protein.

Real time RT-PCR showed a high level of CSGalNAcT-1 expression and lower levels of CSS-1, CSS-2, and CSGlcAT expression in cartilage at E18.5 (Fig. 4*B*, *open bar*); this is consistent with the *in situ* hybridization data. We further

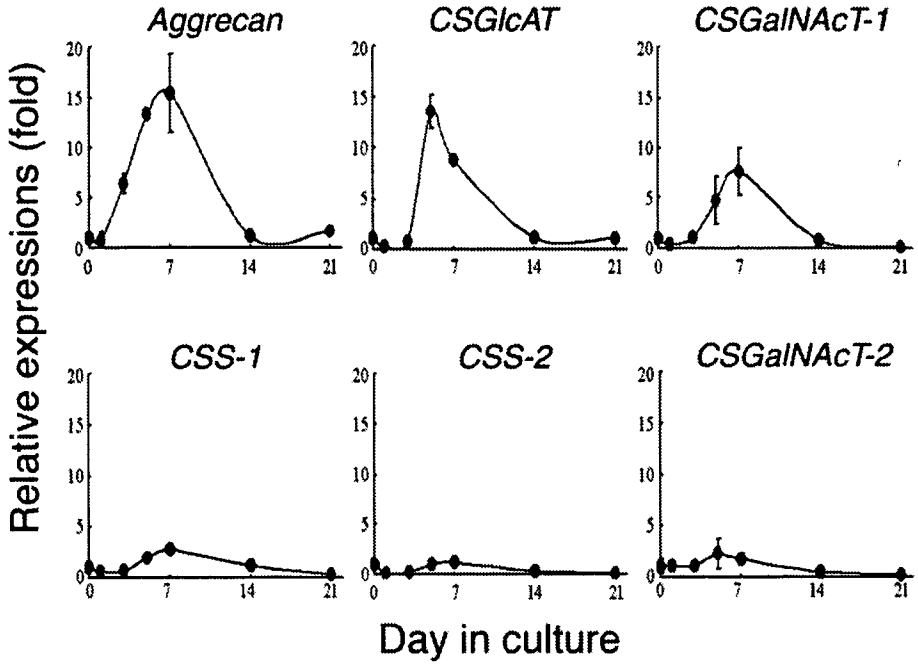

FIGURE 3. **Expression patterns of the glycosyltransferases involved in CS biosynthesis during chondrocyte differentiation of the ATDC5 cells.** The expression levels were standardized with those of glyceraldehyde-3-phosphate dehydrogenase and plotted as a -fold increase against the level at confluence (day 0). Note the correlated expression of CSGlcAT and CSGalNAcT-1 with that of aggrecan core protein.

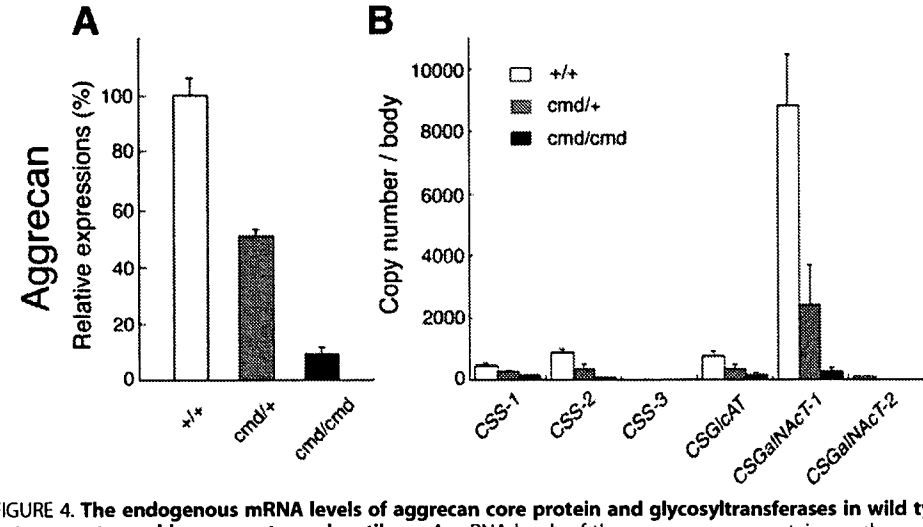

FIGURE 4. **The endogenous mRNA levels of aggrecan core protein and glycosyltransferases in wild type, heterozygote, and homozygote cmd cartilage.** *A*, mRNA levels of the aggrecan core protein are shown as a percentage of wild type E18.5 cartilage. *B*, mRNA levels of glycosyltransferases are shown as the copy number (+/+, wild type; *cmd/+*, heterozygote cmd; *cmd/cmd*, homozygote cmd). Note the high expression of CSGalNAcT-1 and its good correlation with that of aggrecan core protein.

investigated the correlation between CS biosynthetic enzymes and aggrecan expression, using cartilage isolated from mice with cmd, known as natural aggrecan-null mice (32, 33). Since the heterozygote and homozygote cmd cartilage exhibited ~50 and ~9% aggrecan gene transcription, respectively (Fig. 4*A*), quantification of the enzyme expression in the wild type, heterozygote, and homozygote cartilage could facilitate the identification of enzymes critical for CS biosynthesis. In the cmd heterozygote cartilage, CSGalNAcT-1 expression was diminished to ~30% that of the wild type, whereas expression of the other enzymes was constantly low (Fig. 4*B*, *gray bar*). In the cmd homozygote cartilage, CSGalNAcT-1 expression further decreased to a low level similar to that of the other enzymes (Fig. 4*B*, *black bar*). These results, demonstrating high levels of gene expression in cartilage and a good correlation with aggrecan core protein expression, suggested that CSGalNAcT-1 mainly regulates CS synthesis in cartilage.

CSGalNAcT-1 Overexpression Enhances CS Biosynthesis in Chondrocytic Cells—Next, we examined whether CSGalNAcT-1 overexpression could enhance CS biosynthesis in LTC cells. LTC cells are derived from a rat chondrosarcoma and have the characteristics of mature chondrocytes, including a high level of aggrecan expression (34, 35). Cells stably transfected with the CSGalNAcT-1 expression plasmid overexpressed human CSGalNAcT-1 mRNA by ~80-fold compared with endogenous rat mRNA expression (data not shown). Metabolic labeling with [^{35}S]sulfate showed up to a ~2.2-fold increase in CS levels in both the conditioned medium and the cell lysates of the CSGalNAcT-1-overexpressing cells compared with the mock-transfected cells. In contrast, stable clones overexpressing comparable levels of CSS-1, CSS-2, and CSGlcAT did not show increased CS biosynthesis (Fig. 5*A*). A stronger staining intensity with Alcian blue confirmed the increased CS biosynthesis in the CSGalNAcT-1-overexpressing cells (Fig. 5*B*). These results indicate that, whereas the activity of CSS-1, CSS-2, and CSGlcAT in LTC cells is saturated, that of CSGalNAcT-1 is not and that CSGalNAcT-1 overexpression further enhances CS biosynthesis.

Aggrecan in CSGalNAcT-1-overexpressing Cells Contains a Larger Number of CS Chains—Aggrecan core protein expression may have been up-regulated by CSGalNAcT-1 overexpression, as shown by the correlation between the expression in ATDC5 and N1511 cells and that in cmd cartilage. However, real time RT-PCR revealed similar mRNA levels of aggrecan core protein in both CSGalNAcT-1 and mock-transfected LTC cells (Fig. 6*A*). Dot blot analysis showed similar levels of aggrecan core protein in the conditioned media and cell lysates of both transfected cell types (Fig. 6*B*). Since these data suggested that aggrecan synthesized in the CSGalNAcT-1-overexpressing cells contains a larger CS amount per molecule, we examined the density of aggrecan. CsCl density gradient ultracentrif-